

1   **Spatially-distributed influence of agro-environmental factors**  
2   **governing nitrate fate and transport in an irrigated stream-**  
3   **aquifer system**

4

5   **Ryan T. Bailey<sup>1</sup>, Mehdi Ahmadi<sup>2</sup>, Timothy K. Gates<sup>1</sup>, and Mazdak Arabi<sup>1</sup>**

6   [1] {Department of Civil and Environmental Engineering, Colorado State University, 1372  
7   Campus Delivery, Fort Collins, CO, 80523-1372, United States}

8   [2] {Department of Civil Engineering, Sharif University of Technology, Azadi St., Tehran,  
9   11365-11155, Iran}

10   Correspondence to: R. T. Bailey (rtbailey@engr.colostate.edu)

11   Tel: 970-491-5045

12   Fax: 970-491-7727

13

14

15

16

17

18

19

20    **Abstract**

21    Elevated levels of nitrate (NO<sub>3</sub>) in groundwater systems pose a serious risk to human populations  
22    and natural ecosystems. As part of an effort to remediate NO<sub>3</sub> contamination in irrigated stream-  
23    aquifer systems, this study elucidates agricultural and environmental parameters and processes  
24    that govern NO<sub>3</sub> fate and transport at the regional (500 km<sup>2</sup>), local (50 km<sup>2</sup>), and field scales (< 1  
25    km<sup>2</sup>). Specifically, the revised Morris sensitivity analysis method was applied to a finite-  
26    difference nitrogen cycling and reactive transport model of a regional-scale study site in the  
27    Lower Arkansas River Valley in southeastern Colorado. The method was used to rank the  
28    influence of anthropogenic activities and natural chemical processes on NO<sub>3</sub> groundwater  
29    concentration, NO<sub>3</sub> mass leaching, and NO<sub>3</sub> mass loading to the Arkansas River from the  
30    aquifer. Sensitivity indices were computed for the entire study area in aggregate as well as each  
31    canal command area, crop type, and individual grid cells. Results suggest that fertilizer loading,  
32    crop uptake, and heterotrophic denitrification govern NO<sub>3</sub> fate and transport for the majority of  
33    the study area, although their order of influence on NO<sub>3</sub> groundwater concentration and mass  
34    leaching varies according to crop type and command area. Canal NO<sub>3</sub> concentration and rates of  
35    autotrophic denitrification, nitrification, and humus decomposition also dominate or partially  
36    dominate in other locations. Each factor, with the exception of O<sub>2</sub> reduction rate, is the  
37    dominating influence on NO<sub>3</sub> groundwater concentration at one or more locations within the  
38    study area. Results can be used to determine critical processes and key management actions for  
39    future data collection and remediation strategies, with efforts able to be focused on localized  
40    areas.

41

42    **1 Introduction**

43    During recent decades, elevated concentration of nitrate (NO<sub>3</sub>)  $C_{NO_3}$  in groundwater systems and  
44    at points of groundwater discharge to surface water bodies has become a serious environmental  
45    issue due to its adverse effects on human populations and natural ecosystems [Spalding and  
46    Exner, 1993]. Specific problems associated with high  $C_{NO_3}$  include methemoglobinemia for  
47    infants [Fan and Steinberg, 1996] and eutrophication in aquatic systems, which induces depletion

48 of dissolved oxygen (O<sub>2</sub>) (hypoxia) due to increased biological activity. In addition, high  $C_{NO_3}$  can  
49 lead to elevated concentrations of sulfate and selenium (Se) via oxidation of pyrite (FeS<sub>2</sub>) and  
50 seleno-pyrite (FeSe<sub>2</sub>) from marine shale [Frind et al., 1990; Jørgensen et al., 2009; Bailey et al.,  
51 2012]. NO<sub>3</sub> also has been shown to mobilize uranium via oxidation [Wu et al., 2010]. Recent  
52 studies have revealed that certain rock formations can yield nitrogen (N) in response to a variety  
53 of biogeochemical processes [Holloway and Dahlgren 2002, Montross et al 2013]. In most cases,  
54 however, elevated concentrations result from excessive loadings of organic or inorganic N  
55 fertilizer, inducing NO<sub>3</sub> leaching to the saturated zone of the aquifer [Korom, 1992; Spalding and  
56 Exner, 1993].

57 To combat NO<sub>3</sub> contamination, numerous field and modeling studies have been performed to  
58 quantify NO<sub>3</sub> fate and transport processes in soil-groundwater systems, identify baseline  
59 conditions of N sources and transport patterns, and investigate potential remediation strategies.  
60 For the latter, simulation models typically are used to predict the effect of land use and best-  
61 managements practices (BMPs) such as reduction in fertilizer loading [Chaplot et al., 2004;  
62 Almasri and Kaluarachchi, 2007; Lee et al., 2010], reduction in applied irrigation water [Ma et  
63 al., 1998; Rong and Xuefeng, 2011], and implementing or enhancing riparian buffer zones  
64 [Hefting and Klein, 1998; Spruill, 2000; Vaché et al., 2002; Sahu and Gu, 2009] on overall  $C_{NO_3}$ ,  
65 and on NO<sub>3</sub> mass loading to and within streams. These studies have been conducted at various  
66 scales [Ocampo et al., 2006], ranging from the soil profile and field scale [Johnsson et al., 1987;  
67 Ma et al., 1998; Rong and Xuefeng, 2011], to the catchment scale [Birkinshaw and Ewen, 2000;  
68 Conan et al., 2003; Wriedt and Rode, 2006; Lee et al., 2010], to the regional-scale watershed or  
69 river basin scale [Chaplot et al., 2004; Almasri and Kaluarachchi, 2007; Bailey et al., 2015], and  
70 include a variety of fate and transport processes such as soil N cycling, leaching, groundwater  
71 transport, and overland transport.

72 Besides assessing baseline conditions and predicting domain-scale effects on spatial  
73 concentrations and loadings, numerical models also can be used in NO<sub>3</sub> remediation to determine  
74 the system inputs, parameters, and processes (i.e., model factors) that govern these  
75 concentrations and loadings. In general, identifying the most influential processes on resulting  
76  $C_{NO_3}$  and mass loading can assist in establishing optimal remediation strategies. Additional

77 benefits of the analysis include guiding effective field sampling strategies by focusing on  
78 influential system variables or inputs; facilitating model calibration and testing by focusing on  
79 the identified key factors [Sincock et al., 2003; Almasri and Kaluarachchi, 2007]; identifying  
80 factors that require additional research to improve model performance [Hall et al., 2009]; and  
81 detecting non-influential parameters or processes that possibly could be eliminated to simplify  
82 the model [Saltelli et al., 2008].

83 An appealing approach to determine the influence of model factors is sensitivity analysis (SA),  
84 which relates changes in model output variables (e.g., concentration, mass loading) to prescribed  
85 changes in model factor input values (e.g., initial conditions, system stresses, system  
86 parameters). For studies assessing NO<sub>3</sub> fate and transport in groundwater systems using  
87 physically-based spatially-distributed groundwater models, sensitivity analysis typically is  
88 performed in a simple fashion due to model complexity and computational cost. For example,  
89 Almasri and Kaluarachchi [2007] increased values of selected parameters (e.g., denitrification  
90 rate, longitudinal dispersivity, initial concentration, soil mineralization rate, soil nitrification rate,  
91 fertilizer loading) by 50% to determine their influence on simulated  $C_{NO_3}$  in a watershed in  
92 Washington state, USA; Ehteshami et al. [2013], using the LEACHN model, investigated the  
93 influence of low and high values of rainfall and initial  $C_{NO_3}$  for two soil types on soil  $C_{NO_3}$ . In a  
94 field study using the RISK-N model, Oyarzun et al. [2007] modified values of soil initial N,  $C_{NO_3}$   
95 in irrigation water, fertilizer, N crop uptake, crop evapotranspiration (ET), and soil properties by  
96 50%, 70%, 100%, 125%, and 150% to investigate their influence on NO<sub>3</sub> vadose zone mass flux  
97 and  $C_{NO_3}$  in the groundwater. Also, Hartmann et al. [2013] used SA to estimate the influence of  
98 model parameters on the time lag between spring discharge and NO<sub>3</sub> at several karst aquifer sites  
99 across Europe. Whereas global effects of the model factor on system-response variables can be  
100 assessed, local and interaction effects cannot be quantified.

101 A more rigorous SA method is global sensitivity analysis (GSA), which searches the entire  
102 parameter space to identify the importance of model parameters and interactions thereof. Such  
103 methods include the Elementary Effects (EE) method [Morris, 1991; Cacuci, 2003], a screening  
104 method that identifies the most important model factors and is well-suited for large models  
105 [Campolongo and Braddock, 1999], and variance-based methods that quantitatively decompose

106 the variance of model output into fractions that are attributed to model factors [Saltelli et al.,  
107 2008]. A number of hydrologic modeling studies have used GSA methods for assessing model  
108 factor influence on overall watershed nutrient and sediment processes [White and Chaubey,  
109 2005; Arabi et al., 2007; Sun et al., 2012, Ahmadi et al., 2014], flooding and hydraulic  
110 characteristics [Hall et al., 2005; Hall et al., 2009], in-stream water quality [Cox and Whitehead,  
111 2005; Deflandre et al., 2006; Liu and Zou, 2012; Bailey and Ahmadi, 2014], and in-stream solute  
112 transport [Kelleher et al., 2013].

113 Sensitivity analysis is commonly used in hydrologic and water quality modeling to identify the  
114 influence of model parameters on an aggregated measure of model responses such as average  
115 annual stream discharge or contaminant loads. A few studies have assessed how the results of SA  
116 vary in time. For example Reusser et al. [2011] used hydrologic catchment models to investigate  
117 the temporal-varying influence of model factors on a variety of watershed response variables for  
118 catchments in Ecuador and Germany. However, the spatial variability of sensitivity indices has  
119 been largely neglected. Specifically regarding this study, no studies have quantified the spatial-  
120 varying influence of factors on solute concentrations in large-scale groundwater systems. Such  
121 information could be valuable in terms of implementing site-specific remediation strategies,  
122 facilitating model calibration for specific model domain regions, and identifying system  
123 variables that require additional field data collection, particularly for NO<sub>3</sub> due to its ubiquitous  
124 presence in groundwater systems worldwide.

125 This study aims to identify the spatially-varying influence of system factors on NO<sub>3</sub> fate and  
126 transport in a regional-scale (506 km<sup>2</sup>) irrigated hydro-agricultural system. Specifically, the  
127 factors' influence on NO<sub>3</sub> groundwater concentrations, NO<sub>3</sub> leaching below root zone, and NO<sub>3</sub>  
128 groundwater mass loading to the stream network will be quantified for a variety of scales  
129 (cultivated field, canal command area, region). A calibrated and tested N fate and transport  
130 groundwater model is used for the assessment, with the modified Morris method used for the  
131 sensitivity analysis.

132

133

134    **2 Methods**

135    A comprehensive SA method was applied to a regional-scale, intensively irrigated 506 km<sup>2</sup>  
136    groundwater system in the Lower Arkansas River Valley (LARV) in southeastern Colorado to  
137    identify the spatially-varying influence of system factors on NO<sub>3</sub> concentrations in groundwater,  
138    NO<sub>3</sub> mass leaching in the shallow soil zone, and NO<sub>3</sub> mass loading to the Arkansas River. The  
139    model used is UZF-RT3D [Bailey et al., 2013a, 2013b], a MODFLOW [Niswonger et al., 2011]  
140    based, finite-difference model designed for N fate and transport at the regional scale and recently  
141    calibrated and tested for the study area [Bailey et al., 2014]. The model accounts for major  
142    agricultural inputs (fertilizer, canal seepage, irrigation water), processes (N cycling in the root  
143    and soil zone, leaching, three-dimensional transport, heterotrophic and autotrophic  
144    denitrification), and outputs (mass loading to the stream network).

145    As identifying the relative importance of parameters and processes in space is the objective of  
146    this study, and since computational costs of UZF-RT3D are extremely high (run-time of  
147    approximately 3.5 hours for a single simulation using an Intel® Core™ i7-3770 CPU @  
148    3.40GHz desktop computer), the SA method used is an improved variant [Campolongo et al.,  
149    2007] of the Morris method [Morris, 1991] rather than variance-based SA methods such as  
150    Sobol' [Sobol', 1993] or FAST (Fourier Amplitude Sensitivity Test) [Cukier et al., 1973]. Nine  
151    model factors are included in the assessment, with their overall influence on NO<sub>3</sub> fate and  
152    transport evidenced in a previous study in the region [Bailey et al., 2014]. In conjunction with  
153    the SA methodology, model results are processed to determine the dominant model factors  
154    globally (i.e., averaged for the entire model domain), for each irrigation canal command area, for  
155    each crop type (i.e., the set of model grid cells associated with each crop type), and for each grid  
156    cell, thereby elucidating parameter influence at varying spatial scales. For the latter, spatial  
157    contour maps depicting model sensitivity to individual model factors are shown. Due to the  
158    dependence of N fate and transport on the presence of O<sub>2</sub>, the influence of the 9 model input  
159    factors on C<sub>O<sub>2</sub></sub> also is calculated and presented.

160

161

162    **2.1 Study Area**

163    The semi-arid LARV in Colorado extends from the outlet of the Arkansas River from Pueblo  
164    Reservoir eastward across southeastern Colorado to the border with Kansas (Figure 1), with the  
165    Arkansas River fed primarily by snowmelt from the mountainous regions of the upper Arkansas  
166    basin. In total, the valley supports approximately 109,000 irrigated ha (270,000 ac), and is one of  
167    Colorado's most productive agricultural areas. Approximately 14,000 fields are cultivated, with  
168    the majority using flood irrigation methods and a small minority using sprinklers or drip  
169    irrigation methods. Major crops include alfalfa, corn, grass hay, wheat, sorghum, dry beans,  
170    cantaloupe, watermelon, melons, and onions.

171    The region of the LARV focused on in this study is shown in Figure 1. The boundary of the  
172    study area is shown with a black line, and encompasses an area of 50,600 ha (125,000 ac), of  
173    which 26,400 ha (65,300 ac) are irrigated. The fields receiving water from each of six main  
174    irrigation canals (i.e. canal command areas) are shown in Figure 2a, with crop type cultivated in  
175    2006 for each field shown in Figure 2b. Due to over-irrigation and poor subsurface drainage,  
176    high water table elevations have been established in recent decades, with water table depth below  
177    ground surface often between 1-3 m [Morway and Gates, 2012]. These high water tables have  
178    resulted in salinization and waterlogging, in addition to substantial rates of groundwater return  
179    flows (i.e. discharge) to the Arkansas River and its tributaries [Morway et al., 2013]. The  
180    thickness of the alluvial aquifer ranges from 4 to 34 m (Figure 4A), and is underlain by  
181    Cretaceous Shale [Scott, 1968; Sharps, 1976] in both solid and weathered form.

182    In addition to salinization and associated decrease in crop productivity [Morway and Gates,  
183    2012], elevated groundwater  $C_{NO_3}$  has been observed, presumably due to over-fertilization on  
184    cultivated fields. In a similar irrigated region of the LARV, located about 67 km upstream,  
185    Zielinski et al. [1997] examined  $\delta^{15}\text{N}$  isotopic signatures to conclude that NO<sub>3</sub> was derived  
186    primarily from fertilizer and crop waste, not from proximate geologic sources. To assess the  
187     $C_{NO_3}$  in the study region, groundwater and surface water samples were collected (see locations in  
188    Figure 2a) during 10 sampling events over the period 2006-2009 [Gates et al. 2009]. For  
189    groundwater, samples were taken routinely from 52 observation wells, with groundwater from 37

additional observation wells sampled non-routinely (aperiodic). Surface water samples were taken from 10 locations along the Arkansas River and 5 locations in tributaries. Detailed results of the monitoring scheme are shown in Supplementary Data. In summary, for groundwater the 85<sup>th</sup> percentile values of  $C_{NO_3-N}$  were at or in excess of the 10 mg/L (85<sup>th</sup> percentile) EPA drinking water standard for the first three sample trips. The maximum measured value was 66 mg/L. The means for the samples gathered from the Arkansas River and its tributaries were 1.53 mg/L and 1.95 mg/L, respectively. The annual median values of the Arkansas River samples were 0.95, 1.20, 1.10, and 2.20 mg/L for each of the successive years within the period 2006 - 2009, compared to the Colorado interim standard of 2 mg/L [CDPHE, 2012] for total N concentration ( $C_{NO_3-N} + C_{NO_2-N} + C_{NH_4-N}$ ). The concentration of  $C_{NO_3-N}$  exceeded 2 mg/L in about 25% of the samples gathered in the river over this period and exceeded 2.5 mg/L in about 12% of the samples, signifying the growing concern about N pollution in the river. Analysis of 22 river samples and 15 tributary samples in 2013 revealed that  $C_{NO_3-N}$  made up greater than 80% of total dissolved N in the river and about 76% of total dissolved N in the tributaries.

## 2.2 UZF-RT3D N Reaction Module and Baseline Application

UZF-RT3D simulates the reactive transport of multiple interacting chemical species in variably-saturated porous media using groundwater flow rates, water content, and a variety of groundwater sources and sinks (e.g., applied irrigation water, pumping, canal seepage, groundwater-surface water interactions) simulated by a MODFLOW-NWT model using the UZF1 package. The N cycling and reaction module add-on package [Bailey et al., 2013b] was designed for model application in an irrigated agricultural groundwater system, and accounts for the major hydrologic, chemical, and land management processes that govern N fate and transport in an irrigated stream-aquifer system. Also, due to the dependence of N cycling and transport on the presence of O<sub>2</sub>, the fate and transport of O<sub>2</sub> is included.

A schematic of the fate and transport of N species and O<sub>2</sub> as simulated by the N reaction module of UZF-RT3D is depicted in Figure 3A. N mass (NO<sub>3</sub> or NH<sub>4</sub>) enters the subsurface via fertilizer loading (single application or split application), canal seepage, infiltrating irrigation water (either from canal water or pumped groundwater), or seepage from the stream network (Arkansas River

## Environmental Factors Governing $\text{NO}_3$ Transport

218 and its tributaries). N mass exits the subsurface via groundwater discharge to the stream network.  
 219 N cycling occurs in the root and soil zone, with organic N and carbon (C) added to soil organic  
 220 matter (manure  $M_N$ , fast-decomposing litter  $L_N$ , flow-decomposing humus  $H_N$ ) via after-harvest  
 221 plowing or decaying root mass and subsequently mineralized to  $\text{NH}_4$ , which can be volatilized,  
 222 nitrified to  $\text{NO}_3$ , or taken up with  $\text{NO}_3$  into crop roots during the growing season. The timing of  
 223 land management actions, e.g. fertilizer loading (40%, 60% split application), irrigation events,  
 224 harvesting, and plowing, adopted in the module is shown in Figure 3B.  $\text{NH}_4$  is sorbed readily to  
 225 soil surface sites, whereas  $\text{NO}_3$  is transported by one-dimensional transport in the unsaturated  
 226 zone and three-dimensional transport in the saturated zone, subject to heterotrophic  
 227 denitrification in near-surface areas and autotrophic denitrification in the presence of  $\text{FeS}_2$ -  
 228 bearing marine shale (see Figure 1).  $\text{O}_2$  also is subject to heterotrophic and autotrophic chemical  
 229 reduction.

230 UZF-RT3D solves a system of advection-dispersion-reaction (ADR) equations for interacting  
 231 dissolved-phase and solid-phase species using the finite-difference approach. Including ADR  
 232 processes and source/sink terms as depicted, the following mass conservation equations are  
 233 written for the dissolved-phase species ( $\text{NO}_3$ ,  $\text{NH}_4$ ,  $\text{O}_2$ ) in the N reaction module:

$$\frac{\partial(C_{\text{NH}_4}\theta)}{\partial t}R_{\text{NH}_4} = -\frac{\partial}{\partial x_i}(\theta v_i C_{\text{NH}_4}) + \frac{\partial}{\partial x_i} \left( \theta D_{ij} \frac{\partial C_{\text{NH}_4}}{\partial x_j} \right) + q_f C_{f_{\text{NH}_4}} + F_{\text{NH}_4} - U_{\text{NH}_4} + \varepsilon(r_{s,N}^{\text{min}} - r_{s,N}^{\text{imm}}) + \theta(-r_f^{\text{nit}} - r_f^{\text{vol}}) \quad (1)$$

$$\frac{\partial(C_{\text{NO}_3}\theta)}{\partial t} = -\frac{\partial}{\partial x_i}(\theta v_i C_{\text{NO}_3}) + \frac{\partial}{\partial x_i} \left( \theta D_{ij} \frac{\partial C_{\text{NO}_3}}{\partial x_j} \right) + q_f C_{f_{\text{NO}_3}} + F_{\text{NO}_3} - U_{\text{NO}_3} + \theta(r_f^{\text{nit}} - r_{f,\text{NO}_3}^{\text{het}} - r_{f,\text{NO}_3}^{\text{auto}}) \quad (2)$$

$$\frac{\partial(C_{\text{O}_2}\theta)}{\partial t} = -\frac{\partial}{\partial x_i}(\theta v_i C_{\text{O}_2}) + \frac{\partial}{\partial x_i} \left( \theta D_{ij} \frac{\partial C_{\text{O}_2}}{\partial x_j} \right) + q_f C_{f_{\text{O}_2}} + \theta(-r_{f,\text{O}_2}^{\text{het}} - r_{f,\text{O}_2}^{\text{auto}}) \quad (3)$$

234 where  $C$  is solute concentration [ $\text{M L}^{-3}$ ], with  $f$  denoting fluid phase;  $v$  is the pore velocity [ $\text{L b T}^{-1}$ ]  
 235 ], provided by MODFLOW-UZF1;  $\theta$  is the volumetric water content [ $\text{L}^3 \text{L}^{-3}$ ], also provided by  
 236 MODFLOW-UZF1;  $D_{ij}$  is the hydrodynamic dispersion coefficient [ $\text{L}^2 \text{T}^{-1}$ ];  $q_f$  is the volumetric

237 flux of water representing sources and sinks [ $L_f^3 T^{-1} L_b^{-3}$ ] such as irrigation water, canal and river  
 238 seepage, groundwater discharge to the river, or pumped groundwater, with  $b$  denoting the bulk  
 239 phase;  $C_f$  is the concentration of the source or sink [ $M_f L_f^{-3}$ ];  $F$  is the inorganic fertilizer  
 240 application [ $M_f L_b^{-3} T^{-1}$ ];  $U$  is the potential crop uptake rate [ $M_f L_b^{-3} T^{-1}$ ];  $\varepsilon$  is the volumetric solid  
 241 content [ $L_s^3 L_b^{-3}$ ] with  $s$  denoting the solid phase, and is equal to  $1 - \phi$ , where  $\phi$  is porosity [ $L_f^3 L_b^{-3}$ ];  
 242  $r_f$  represents the rate of all reactions that occur in the dissolved-phase [ $M_f L_f^{-3} T^{-1}$ ]; *min*, *imm*,  
 243 *nit*, and *vol* signify mineralization, immobilization, nitrification, and volatilization of NH<sub>4</sub>,  
 244 respectively; and *auto* and *het* represent autotrophic and heterotrophic chemical reduction,  
 245 respectively.  $\varepsilon$  is included for the min and imm reactions to denote a mass transfer between the  
 246 solid and dissolved phases. For NH<sub>4</sub>, which is subject to sorption,  $R$  is the retardation factor and  
 247 is equal to  $1 + (\rho_b K_{d, \text{NH}_4})/\theta$ , where  $\rho_b$  is the bulk density of the porous media [ $M_b L_b^{-3}$ ] and  
 248  $K_{d, \text{NH}_4}$  is the partitioning coefficient [ $L_f^{-3} M_b$ ]. The daily mass of potential N crop uptake during  
 249 the growing season is determined using a logistic equation [Johnsson et al., 1987] and is  
 250 distributed across the vertical column of grid cells encompassing the crop rooting depth  
 251 according to the mass density of the root system. Mass conservation equations (not shown) for  
 252 solid-phase organic N (and C) species L<sub>N</sub>, H<sub>N</sub>, and M<sub>N</sub> also are implemented.

253 The rate of chemical reactions  $r_f$  included in Equations (1-3) is governed by the dependence of  
 254 the chemical reaction on soil temperature  $T$ ,  $\theta$ , and the presence of O<sub>2</sub> and C. These rates are  
 255 simulated using first-order Monod kinetics. For example, the following rate law expression  
 256 represents the process of heterotrophic denitrification, with others contained in Bailey et al.  
 257 [2015]:

$$r_{f, \text{NO}_3}^{\text{het}} = \lambda_{\text{NO}_3}^{\text{het}} C_{\text{NO}_3} \left( \frac{C_{\text{NO}_3}}{K_{\text{NO}_3} + C_{\text{NO}_3}} \right) \left( \frac{CO_{2, \text{prod}}}{K_{CO_2} + CO_{2, \text{prod}}} \right) \left( \frac{I_{O_2}}{I_{O_2} + C_{O_2}} \right) E \quad (4)$$

258 where  $\lambda$  is the base rate constant for the reaction [ $T^{-1}$ ];  $K_j$  is the Monod half-saturation constant  
 259 for species  $j$  [ $M_f L_f^{-3}$ ];  $I_{O_2}$  is the O<sub>2</sub> inhibition constant [ $M_f L_f^{-3}$ ] signifying the species concentration  
 260 at which lower-redox species can undergo appreciable rates of reduction;  $CO_{2, \text{prod}}$  is the total  
 261 mass of CO<sub>2</sub> produced during organic matter decomposition and is used as an indicator of

262 available organic carbon (OC) for microbial consumption [Birkinshaw and Ewen, 2000]; and  $E$   
263 [-] is an environmental reduction factor that accounts for  $\theta$  and  $T$  and acts to temper microbial  
264 activity rates [Birkinshaw and Ewen, 2000; Bailey et al., 2013b]. Nitrification, mineralization,  
265 and denitrification each have uniquely specified relationships between  $\theta$  and microbial activity.

266 The UZF-RT3D model used in this study is the same as that described in Bailey et al. [2014].  
267 The model uses output from a calibrated and tested MODFLOW-NWT [Niswonger et al., 2011]  
268 model of the study region [Morway et al., 2013], which uses the UZF1 unsaturated-zone flow  
269 package [Niswonger et al., 2006]. The flow model uses weekly estimates of irrigation water,  
270 precipitation, canal seepage, crop ET to estimate groundwater level and groundwater-surface  
271 water interactions for the 1999-2009 time period. Figures 4b, 4c, and 4d show the finite-  
272 difference grid, the simulated water content of the soil in June 2006, and the average simulated  
273 water table elevation (m) during the 1999-2009 time period, respectively.

274 The UZF-RT3D model uses the same model domain and finite difference grid as the flow model  
275 (see Figure 4B). The model has 7 vertical layers, with Layers 1-2 (0.5 m each) corresponding to  
276 the root zone, Layer 3 (1.0 m) corresponding to the leaching zone, Layers 4-6 to the saturated  
277 zone, and Layer 7 to the shale bedrock formation. Thickness of layers 4, 5, and 6 varies  
278 according to saturated thickness, with layer thickness ranging from 2.8 m to 12.6 m. Each  
279 vertical column of cells in the 3D grid is assigned a set of crop parameter values according to the  
280 portions of fields within the grid cell area. Crop parameters, with values shown in Table 1 for  
281 each crop type in the study area, include: Planting Day; Harvest Day; Plowing Day; mass of  
282 stover plowed into the soil  $P_{St}$  (kg/ha) after harvest; maximum rooting depth  $d_{rt,max}$  (m), which  
283 controls N uptake; C-N ratio of root mass  $CN_{RT}$ ; fertilizer loading  $F_{NH_4}$  (kg/ha), maximum  
284 seasonal uptake values of N  $N_{up}$  (kg/ha), depth of plowing  $d_{pw}$  (m); mass of decaying roots  $P_{Rt}$   
285 (kg/ha); C-N ratio of stover mass  $CN_{ST}$ ; and constants defining root growth and daily uptake rate  
286  $U$ . Chemical reaction parameter values are shown in Table 2, with an asterisk \* indicating the  
287 mean value of all the grid cells.  $C_{NO_3}$  and  $C_{O_2}$  of canal water and irrigation water were based on  
288 observed data. The model was run for the 2006-2009 and tested against spatio-temporal averages  
289 of groundwater  $C_{NO_3}$  and NO<sub>3</sub> mass loadings from the aquifer to the Arkansas River.

290 **2.3 Assessing Major Controls on NO<sub>3</sub> Fate and Transport**

291 **2.3.1 Morris SA Methodology**

292 The Morris screening method for global SA is based on an individually randomized one-at-a-  
293 time (OAT) design that provides information regarding (i) the main effect of each input  
294 parameter on model output responses and (ii) the overall effects including interactions between  
295 parameters. For example, consider a model  $M$  with a vector of  $k$  parameters ( $\omega_i, i = 1, \dots, k$ ) within  
296 the feasible parameter space,  $\Omega$ , that simulates  $m$  response vectors of the system ( $S_j, j = 1, \dots, m$ ):

$$[S_1, \dots, S_m] = M(\omega_1, \dots, \omega_k) \quad (5)$$

297 Similar to any standard SA practice, parameters are drawn from their predefined distributions,  
298 with each model input parameter  $\omega_i$  varied across  $p$  discrete values [Saltelli et al., 2008]. After  
299 running model  $M$  for the given parameter sets, the local sensitivity measure (also referred to as  
300 the *elementary effect*,  $EE$ ) is then computed for each parameter  $i$  for model response  $j$  as follows:

$$EE_{i,j}(\omega) = \left( \frac{S_j(\omega_1, \dots, \omega_{i-1}, \omega_i + \Delta, \dots, \omega_k) - S_j(\omega)}{\Delta} \right) \quad (6)$$

301 where  $\Delta$  is a value in the predefined increments (i.e.  $[1/(p-1), \dots, 1-1/(p-1)]$ ) and  $\omega =$   
302  $\omega_1, \dots, \omega_k$  is a random sample in the parameter space so that the transformed point  
303  $(\omega_1, \dots, \omega_{i-1}, \omega_i + \Delta, \dots, \omega_k)$  is still within the parameter space  $\Omega$  [Saltelli et al., 2008]. The  
304 resulting distribution  $EE_i$  associated with each parameter  $\omega_i$  is then analyzed to determine  $\mu$ , the  
305 mean of the distribution which assesses the overall importance of the parameter on the model  
306 output; and  $\sigma$ , the standard deviation of the distribution, which indicates non-linear effects and/or  
307 interactions [Campolongo et al., 2007].

308 To determine sensitive and insensitive values, it is recommended to evaluate a graphical  
309 representation of  $\sigma$  vs.  $\mu$ . However, for non-monotonic models, some  $EE$  values with opposite  
310 signs may cancel out when  $\mu$  is calculated, and hence Campolongo and Saltelli [1997] proposed

311 the use of  $\mu^*$ , the sample mean of the distribution of absolute values of  $EE$ .  $\mu^*$  includes all types  
 312 of effects that parameters can have on output responses and, therefore, is a global measure of  
 313 output sensitivity to the parameters [Campolongo et al., 2007].  $\mu_{i,j}^*$  is defined as the mean of  
 314 absolute values of the computed elementary effects  $EE_{i,j}$ . The total computational cost of the  
 315 Morris experiment is  $n = r(k+1)$  runs, where  $r$  is the selected size of each sample.

316 As noted above, an important objective of SA is to determine the most influential model input  
 317 parameters. Hence, it is important to measure the level of agreement between results of SA  
 318 experiments with an emphasis on the high-ranked parameters. Campolongo and Saltelli [1997]  
 319 suggested the use of the Savage score to facilitate comparison of results from different SA  
 320 experiments (see next section). The Savage score is defined as follows [Iman and Conover,  
 321 1987]:

$$SS_i = \sum_{h=i}^k \frac{1}{h} \quad (7)$$

322 where  $i$  is the rank assigned to the  $i^{\text{th}}$  model parameter based on the Morris  $\mu^*$ . For example, the  
 323 highest ranked variable would have a score of  $1/1 + 1/2 + 1/3 + \dots + 1/k$ . The second ranked  
 324 variable would have a score of  $1/2 + 1/3 + \dots + 1/k$ , and so on. Savage scores typically are  
 325 preferred because they place higher emphasis on the agreement of the key drivers (i.e. higher  
 326 ranked parameters), rather than the overall agreement. The Savage score can be used in  
 327 aggregating the results from different SA methods.

### 328 **2.3.2 Model Input Factors Analyzed**

329 In applying the SA method to the UZF-RT3D model of the study area, 9 model input factors  
 330 were analyzed for impact on model results:  $F_{NH_4}$ ,  $N_{up}$ ,  $C_{NO_3}$  in canal water  $Canal_{NO_3}$ , rate of litter  
 331 pool decomposition  $\lambda_L$ , rate of humus pool decomposition  $\lambda_H$ , rate of autotrophic reduction of O<sub>2</sub>  
 332 in the presence of shale  $\lambda_{O_2}^{auto}$ , rate of autotrophic reduction of NO<sub>3</sub> in the presence of shale  $\lambda_{NO_3}^{auto}$ ,  
 333 rate of nitrification  $\lambda_{nit}$ , and rate of heterotrophic denitrification  $\lambda_{NO_3}^{het}$ .  $Canal_{NO_3}$  conveys NO<sub>3</sub> mass  
 334 into the subsurface system via applied irrigation water as well as seeped canal water. For each

335 simulation, separate values of  $F_{NH_4}$  and  $N_{up}$  were generated for each crop type, separate values of  
336  $Canal_{NO_3}$  were generated for each of the six canal command areas, and separate values of  $\lambda_{O_2}^{auto}$ ,  
337  $\lambda_{NO_3}^{auto}$ , and  $\lambda_{nit}$  were generated for each command area. The mean of each parameter value is  
338 derived from the baseline simulation (see Tables 1 and 2), with the mean values of  $\lambda_{O_2}^{auto}$ ,  $\lambda_{NO_3}^{auto}$ ,  
339 and  $\lambda_{nit}$  for each command area estimated during the calibration phase [Bailey et al., 2014].

340 Setting the number of replications  $r$  and levels  $p$  of the Morris scheme to 20 and 10, respectively,  
341 a total of 280 simulations were run. Parameter values were perturbed using a coefficient of  
342 variation (CV) of 0.2 for all parameters except for  $Canal_{NO_3}$ , which was perturbed with a CV of  
343 0.1 based on variance in observed canal water concentrations. Perturbation for the reaction rates  
344 ( $\lambda_L$ ,  $\lambda_H$ ,  $\lambda_{O_2}^{auto}$ ,  $\lambda_{NO_3}^{auto}$ ,  $\lambda_{NO_3}^{het}$ ,  $\lambda_{nit}$ ) was performed using log values since statistically these rates  
345 typically conform to a lognormal distribution [Parkin and Robinson, 1989; McNab and Dooher,  
346 1998]. CV values were selected by comparing the resulting spread of parameter values to values  
347 found in the literature and from field data in the study area. The values of  $F_{NH_4}$ ,  $\lambda_{NO_3}^{auto}$ , and  
348  $Canal_{NO_3}$  for each of the 280 simulations are shown in Figure 5, with averages of 250 kg/ha,  
349  $1.055 \times 10^{-4}$  day<sup>-1</sup>, and 2.6 g m<sup>-3</sup>, respectively. The values shown in Figure 5A are for grid cells  
350 that contain corn, and the values shown in Figures 5B and 5C are for the grid cells within the  
351 Rocky Ford Highline canal command area (canal feeding the gray-shaded fields in Figure 2A).

352 For each of the 280 simulations, the model was run for a 2-year spin-up period, followed by the  
353 2006-2009 period. Model results were processed to determine the influence of the 9 targeted  
354 model input factors on groundwater  $C_{NO_3}$ , NO<sub>3</sub> mass leached from the root zone, and total NO<sub>3</sub>  
355 mass loading to the Arkansas River from the aquifer. Post-processing was implemented to  
356 determine this influence (i) globally for the entire study area, i.e. averaging values from all grid  
357 cells; (ii) for individual crop types, i.e. averaging values from all grid cells corresponding to a  
358 given crop type; (iii) for individual canal command areas, i.e. averaging values from all grid cells  
359 within a given command areas; and (iv) for individual grid cells. As total NO<sub>3</sub> mass loading to  
360 the Arkansas River occurs along the entire reach of the river within the study area, parameter  
361 influence is assessed only for (i). Values of average concentration, average leaching, and total

362 mass loading were processed from the final year of the model simulation (i.e. 2009). For  
363 groundwater  $C_{NO_3}$ , concentration values were taken from Layer 4 of the model, which  
364 corresponds to the depth of observation well screens in the study area. For NO<sub>3</sub> leaching, values  
365 are taken from Layer 3 (i.e. the mass leached from Layer 3 to Layer 4). For parameter influence  
366 on  $C_{NO_3}$  for individual grid cells (item iv), the Savage score as calculated by Equation (7) will be  
367 used for presentation of results. Also for (iv), the parameter influence on  $C_{O_2}$  will be presented.

368

369 **3 Results and Discussion**

370 **3.1 General Model Results**

371 Model results from one of the 280 simulations is shown in Figure 6, with spatial distribution of  
372  $C_{O_2}$  and  $C_{NO_3}$  shown in Figures 6A and 6B, respectively for July 22, 2009, and the spatial  
373 distribution of NO<sub>3</sub> mass loading shown for one week during the winter (December 2 2006,  
374 Figure 6C) and one week during the summer (August 10 2008, Figure 6D). Mass loadings from  
375 the aquifer to the stream network (discharge) are displayed in red, whereas loadings from the  
376 stream network to the aquifer (seepage) are displayed in green. For concentrations in  
377 groundwater, values of  $C_{O_2}$  range from 0.0 to 10.3 mg/L, with an average value of 2.7 g m<sup>-3</sup> for  
378 the 7,776 active grid cells. Values of  $C_{NO_3}$  range from 0.0 to 78.3 mg/L, with an average value of  
379 1.84 mg/L.

380 Hotspots occur for both  $C_{O_2}$  and  $C_{NO_3}$ , with those of  $C_{NO_3}$  typically occurring in locations of corn  
381 cultivation due to the higher loading of  $F_{NH_4}$  as compared to other crop types. NO<sub>3</sub> mass loadings  
382 occur along the Arkansas River and the tributaries, with discharge and seepage both occurring  
383 along the length of the canals during the summer (Figure 6D). The spatio-temporal average value  
384 of  $C_{NO_3}$  in groundwater for each command area during the entire 2006-2009 time period is shown  
385 in Figure 7 for each of the 280 simulations. The average value for all grid cells in non-cultivated  
386 area also is shown. Average  $C_{NO_3}$  across all simulations for each command area are (average of

387 observed field values are in parentheses) Highline 2.0 mg/L (3.1 mg/L); Catlin: 1.4 mg/L (6.1  
388 mg/L); Rocky Ford: 1.5 mg/L (3.8 mg/L); Fort Lyon: 3.7 mg/L (1.6 mg/L); Holbrook: 1.9 mg/L  
389 (3.5 mg/L); and non-cultivated areas: 3.5 mg/L (4.2 mg/L). Average values correspond closely to  
390 results from the tested baseline model [Bailey et al., 2014].

391 **3.2 Parameter influence on global concentration, leaching, and loading of NO<sub>3</sub>**

392 The global influence of the 9 model input factors on NO<sub>3</sub> fate and transport in the study area is  
393 shown in Figure 8. Global sensitivity plots are used, with non-linear effects and/or interactions  $\sigma$   
394 plotted against mean  $\mu^*$ . The influence of the factors on  $C_{NO_3}$  in Layer 1 (top 0.5 m of the root  
395 zone),  $C_{NO_3}$  in Layer 4 (shallow saturated zone), NO<sub>3</sub> leaching from Layers 3 to 4  $L_{NO_3Lay3 \rightarrow 4}$   
396 (generally from the unsaturated zone to the saturated zone), and total NO<sub>3</sub> mass loading to the  
397 Arkansas River  $Load_{NO_3}$  are shown in Figures 8A, 8B, 8C, and 8D, respectively. As seen in  
398 Figure 8A,  $C_{NO_3}$  in the root zone is governed principally by fertilizer loading ( $F_{NH_4}$ ) and seasonal  
399 NO<sub>3</sub> uptake by crops ( $N_{up}$ ) and to a smaller degree by heterotrophic denitrification ( $\lambda_{NO_3}^{het}$ ) and  
400 nitrification ( $\lambda_{nif}$ ). In the shallow saturated zone (Figure 8B), where NO<sub>3</sub> mass is received from  
401 the upper soil zone via leaching,  $F_{NH_4}$  and  $N_{up}$  still are dominant, but the concentration of NO<sub>3</sub> in  
402 the canals ( $Canal_{NO_3}$ ) has a stronger direct impact than  $\lambda_{NO_3}^{het}$ . The rate of humus decomposition ( $\lambda_H$ )  
403 and autotrophic denitrification ( $\lambda_{NO_3}^{auto}$ ) also have a slight impact. NO<sub>3</sub> leaching also is  
404 governed by  $F_{NH_4}$ ,  $N_{up}$ ,  $\lambda_{NO_3}^{het}$ ,  $Canal_{NO_3}$ , and  $\lambda_H$  (Figure 8C), as higher  $F_{NH_4}$ , lower  $N_{up}$ , lower  
405  $\lambda_{NO_3}^{het}$ , and higher  $Canal_{NO_3}$  increase the mass of NO<sub>3</sub> leached, and vice versa.  $Load_{NO_3}$  is governed  
406 by  $F_{NH_4}$ ,  $N_{up}$ , and  $\lambda_{NO_3}^{het}$  (Figure 8D), with  $\lambda_{NO_3}^{het}$  influencing not only how much NO<sub>3</sub> is leached to  
407 the water table and carried to the stream network via groundwater flow, but also how much NO<sub>3</sub>  
408 undergoes denitrification in the riparian areas of the stream network.

409 The high  $\sigma$  values for  $N_{up}$ ,  $F_{NH_4}$ ,  $\lambda_{NO_3}^{het}$  and  $Canal_{NO_3}$  shown in Figure 8 signify the large spread in  
410  $EE$  values for these parameters, indicating that their influence on  $C_{NO_3}$ , NO<sub>3</sub> leaching, and NO<sub>3</sub>  
411 mass loading is strongly dependent on the values of other parameters. For example, in reference

412 to  $C_{NO_3}$  in the shallow saturated zone (Figure 8B), the value of  $\mu^*$  for  $N_{up}$  signifies the average  
413 effect of  $N_{up}$  on  $C_{NO_3}$ , but some values of  $EE$  for  $N_{up}$  are much smaller and larger than  $\mu^*$ .  
414 Smaller values of  $EE$  indicate that the combined influence of other parameter values produced a  
415 small effect of crop uptake on  $C_{NO_3}$ , such as a lower N fertilizer loading and higher rates of  
416 denitrification, whereas larger values indicate that other parameters produced a larger effect of  
417 crop uptake on  $C_{NO_3}$ , such as a higher N fertilizer loading and lower rates of denitrification. Also,  
418 higher values of  $Canal_{NO_3}$  increase the influence of crop uptake on  $C_{NO_3}$ , as more NO<sub>3</sub> mass is  
419 brought into the soil zone via canal seepage and infiltrating irrigation water.

420 **3.3 Parameter influence on  $C_{NO_3}$  and leaching for each crop type**

421 The influence of each of the 9 parameters on  $C_{NO_3}$  in the shallow groundwater zone and on NO<sub>3</sub>  
422 leaching for each crop type in the study area is summarized in Tables 3 and 4, respectively using  
423 values of  $\mu^*$ . The  $\mu^*$  values of the 3 most influential parameters for each crop type are bolded.  
424 For the majority of crop types,  $C_{NO_3}$  in the shallow groundwater zone is governed by N fertilizer  
425 loading ( $F_{NH_4}$ ), seasonal crop N uptake ( $N_{up}$ ), and heterotrophic denitrification  $\lambda_{NO_3}^{het}$  (Table 3),  
426 similar to the global analysis of  $C_{NO_3}$  in the shallow soil layers as presented in Section 3.2. For  
427 example,  $\mu^*$  for  $F_{NH_4}$ ,  $N_{up}$ , and  $\lambda_{NO_3}^{het}$  is 0.94, 0.72, and 0.30, respectively, for corn-cultivated  
428 areas, and 0.84, 0.81, and 0.28 for sorghum-cultivated areas. The exception is areas that cultivate  
429 onion, in which  $Canal_{NO_3}$  ( $\mu^* = 0.45$ ) ranks in the top three behind  $F_{NH_4}$  (1.21) and  $N_{up}$  (0.99). For  
430 many of the crops,  $\lambda_H$  and  $\lambda_{nit}$  have a small to moderate influence, whereas litter pool  
431 decomposition rate ( $\lambda_L$ ), autotrophic reduction of O<sub>2</sub> ( $\lambda_{O_2}^{auto}$ ), and autotrophic denitrification (  
432  $\lambda_{NO_3}^{auto}$ ) have a negligible to small influence on  $C_{NO_3}$ .

433 The influence of the 9 parameters on NO<sub>3</sub> mass leaching to the shallow saturated zone (Table 4)  
434 follows the same pattern as for their influence on  $C_{NO_3}$ , with fertilizer N loading, uptake, and  
435 denitrification dictating the amount of NO<sub>3</sub> leached to the water table (values in boxes) and canal  
436 concentration, nitrification, and humus and litter pool decomposition having small to moderate

437 values of  $\mu^*$ . For corn-cultivated areas, the average effect  $\mu^*$  of  $F_{NH_4}$ ,  $N_{up}$ , and  $\lambda_{NO_3}^{het}$  is 486.3,  
438 366.8, and 172.3, respectively, compared to 51.3 for  $\lambda_H$ , 41.3 for  $Canal_{NO_3}$ , and 26.4 for  $\lambda_L$ , with  
439 15.2, 1.0, and 0.2 for  $\lambda_{nit}$ ,  $\lambda_{NO_3}^{auto}$ , and  $\lambda_{O_2}^{auto}$ , respectively. Again,  $Canal_{NO_3}$  is the third most  
440 influential parameter for onion-cultivated areas, with  $\mu^* = 1.6$ , compared to 9.7 and 7.2 for  $F_{NH_4}$   
441 and  $N_{up}$ , respectively.

442 **3.4 Parameter influence on  $C_{NO_3}$  and leaching in individual canal command areas**

443 Summaries of the influence of each of the 9 parameters on  $C_{NO_3}$  in the shallow groundwater zone  
444 and on NO<sub>3</sub> leaching for each canal command area also are provided in Tables 3 and 4. The  
445 results show importance differences between the command areas, with a mixture of  $F_{NH_4}$ ,  $N_{up}$ ,  
446  $\lambda_{nit}$ ,  $\lambda_{NO_3}^{het}$ ,  $\lambda_{NO_3}^{auto}$ , and  $Canal_{NO_3}$  providing noteworthy impacts on  $C_{NO_3}$  and NO<sub>3</sub> mass leaching. For  
447 influence on  $C_{NO_3}$  (Table 3), the top three influential parameters within the Catlin command area  
448 are  $N_{up}$  ( $\mu^* = 0.26$ ),  $\lambda_{nit}$  (0.16), and  $F_{NH_4}$  (0.12), whereas the top three for the Rocky Ford  
449 command area are  $Canal_{NO_3}$  (0.51),  $\lambda_{NO_3}^{auto}$  (0.20), and  $N_{up}$  (0.15), with the strong influence of  $\lambda_{NO_3}^{auto}$   
450 due to the presence of outcropped shale in the command area and hence locations of autotrophic  
451 denitrification.  $\lambda_{NO_3}^{auto}$  also has a strong influence in the Holbrook command area, with the third  
452 highest value of  $\mu^*$  (0.11).  $Canal_{NO_3}$  is ranked 3<sup>rd</sup> or higher in terms of  $\mu^*$  in 3 of the 6 command  
453 areas (Rocky Ford, Otero, Highline).  $F_{NH_4}$ ,  $N_{up}$ , and  $\lambda_{NO_3}^{het}$  govern NO<sub>3</sub> mass leaching for each of  
454 the command areas (Table 4) except for the Catlin command area, in which  $\lambda_{nit}$  is ranked second  
455 ( $\mu^* = 38.0$ ) and the Rocky Ford Ditch, in which  $Canal_{NO_3}$  is ranked first ( $\mu^* = 30.3$ ).

456 **3.5 Spatial distribution of parameter influence on  $C_{NO_3}$  and  $C_{O_2}$**

457 Cell-by-cell plots of Savage scores for the parameters according to their ranking in influencing  
458  $C_{NO_3}$  in shallow groundwater are shown in Figure 9. Plots are presented for each of the targeted 9  
459 parameters except for  $\lambda_{O_2}^{auto}$  due to the negligible influence of O<sub>2</sub> autotrophic reduction on  $C_{NO_3}$ .

460 The value for each cell represents the ranking (1-9) and associated Savage score for the given  
461 parameter. High ranking is displayed in maroon-red coloring, whereas low ranking is displayed  
462 in blue. As seen in the plots, the ranking of each parameter in its influence on groundwater  $C_{NO_3}$   
463 is highly spatially-variable. For example, the locations where canal NO<sub>3</sub> concentration ( $Canal_{NO_3}$ )  
464 has the strongest influence (maroon coloring) (Figure 9B) are scattered throughout the region,  
465 with entire local areas (encompassed by circles in Figure 9B) governed by this parameter. For the  
466 cultivated areas, the dominant inputs/processes are fertilizer loading (Figure 9A), crop N uptake  
467 (Figure 9D), and heterotrophic denitrification ( $\lambda_{NO_3}^{het}$ ) (Figure 9E), with humus decomposition  
468 (Figure 9G) having a moderate influence and litter decomposition (Figure 9H) having a small  
469 influence. Whereas fertilizer loading and N uptake have the most influence on  $C_{NO_3}$  in most of the  
470 cultivated areas, some areas are governed principally by heterotrophic denitrification and humus  
471 decomposition (cells colored in maroon in Figures 9E and 9G). Denitrification is particularly  
472 important in riparian areas along tributaries and the Arkansas River (Figure 9E), where dense  
473 vegetation provides a natural filter of NO<sub>3</sub> before being loaded to surface water. Values of humus  
474 decomposition ( $\lambda_H$ ) and litter decomposition ( $\lambda_L$ ) control the rate of organic C and organic N  
475 decomposition and hence the availability of C for heterotrophic denitrification to proceed.

476 No area has  $\lambda_L$  being the dominant influence on  $C_{NO_3}$ . Nitrification rate has a strong impact on  
477  $C_{NO_3}$  in the Holbrook command area (red-pink cell coloring in Figure 9C), with small impact  
478 elsewhere in the study area. Autotrophic denitrification is the dominant parameter in areas along  
479 the Arkansas River and several of the tributaries (Figure 9F) that are adjacent to shale formations  
480 (see Figure 1). However, it is interesting to note that there are many locations in the study area  
481 adjacent to outcropped shale in which  $\lambda_{NO_3}^{auto}$  is not the dominant parameter. These locations are  
482 indicated by circles in Figure 9F. In these areas, other system inputs and processes such as  $F_{NH_4}$ ,  
483  $N_{up}$ ,  $\lambda_{NO_3}^{het}$  and  $\lambda_H$  are the governing influences on  $C_{NO_3}$ , demonstrating that knowledge of shale  
484 locations alone cannot be used to determine where  $C_{NO_3}$  will be affected the most by autotrophic  
485 denitrification.

486 Similar cell-by-cell plots of parameter Savage scores are shown in Figure 10 for influence on  
487  $C_{O_2}$  in shallow groundwater.  $\lambda_H$  and  $\lambda_L$  govern  $C_{O_2}$  in the cultivated areas (Figures 10C,D), with  
488  $F_{NH_4}$  (Figure 10B),  $N_{up}$  (Figure 10E) and  $Canal_{NO_3}$  (Figure 10A) exhibiting small to moderate  
489 influence on  $C_{O_2}$  in the cultivated areas. The strong influence of  $\lambda_H$  and  $\lambda_L$  occurs due to their  
490 control of the rate of organic C decomposition, and hence the availability of C for heterotrophic  
491 reduction of O<sub>2</sub>. The rate of autotrophic reduction of O<sub>2</sub> ( $\lambda_{O_2}^{auto}$ ) is dominant in localized areas  
492 where shale is present (see maroon-shaded cells in Figure 10F) with small influences in other  
493 areas of the study region, mainly in areas down-gradient of the shale areas.

494

#### 495 **4 Discussion of Results**

496 Results provide information regarding the system inputs and processes that control NO<sub>3</sub> fate and  
497 transport generally (across the entire study region), by crop type, by canal command area, and by  
498 local regions. For the entire study region, detailed field sampling and observation of N fertilizer  
499 loading, N crop uptake, heterotrophic denitrification in the shallow soil layers, and concentration  
500 of NO<sub>3</sub> in canal water must be performed as often as possible to provide accurate model input  
501 data. NO<sub>3</sub> in canal water not only seeps through the perimeter of the earthen irrigation canals into  
502 the aquifer, but also is loaded to cultivated fields via applied irrigation water. In addition, results  
503 indicate these inputs and processes must be controlled via implemented management practices if  
504 NO<sub>3</sub> groundwater concentration, NO<sub>3</sub> leaching, and NO<sub>3</sub> mass loading to the river network are  
505 expected to decline in future decades, whereas other processes (organic N decomposition,  
506 nitrification of NH<sub>4</sub>) are not critical target factors.

507 These results agree with other previous studies from regions worldwide, which indicated that key  
508 controls on NO<sub>3</sub> fate and transport in groundwater and watershed systems, and hence targets for  
509 management action, include N fertilizer application [Chaplot et al., 2004; Botter et al., 2006;  
510 Almasri and Kaluarachchi, 2007; Arabi et al., 2007; Bailey et al., 2015] and rate of  
511 denitrification [Wriedt and Rode, 2006; Almasri and Kaluarachchi, 2007; Schilling et al., 2007],  
512 with the order of their influence varied depending on the study region. However, these studies

513 did not analyze the influence of NO<sub>3</sub> in canal irrigation water or the influence of crop N uptake.  
514 Molénat and Gascuel-Odoux [2002] did demonstrate the strong influence of NO<sub>3</sub> leaching on in-  
515 stream NO<sub>3</sub> concentration, similar to our assessment of N uptake and denitrification (which  
516 influence NO<sub>3</sub> leaching) on NO<sub>3</sub> loading from the aquifer to the stream network.

517 The same system parameters that govern NO<sub>3</sub> fate and transport at the regional scale also govern  
518 NO<sub>3</sub> for each individual crop type. N fertilizer loading (less), N crop uptake (more), and  
519 heterotrophic denitrification (more) typically must be controlled to decrease groundwater NO<sub>3</sub>  
520 concentration and NO<sub>3</sub> leaching, with NO<sub>3</sub> concentration in canal water controlled to lower these  
521 values for onion-cultivated areas. For canal command areas, N fertilizer loading and N uptake  
522 must be managed to decrease groundwater NO<sub>3</sub> concentration and NO<sub>3</sub> mass leaching in the  
523 majority of command areas. However, nitrification of NH<sub>4</sub> is an important control for the Catlin  
524 command area, NO<sub>3</sub> concentration in canal water is important for the Highline, Otero, and Rocky  
525 Ford command areas, heterotrophic denitrification is important for each command area except  
526 Catlin and Rocky Ford Ditch, and autotrophic denitrification is important for only the Holbrook  
527 and Rocky Ford Ditch command areas. These reaction rate parameters must be focused on in  
528 field data monitoring scheme and in model parameter estimation. Results demonstrate that  
529 targeted inputs/outputs and processes vary depending on command area.

530 Similarly, different targets are required for controlling NO<sub>3</sub> fate and transport in localized areas  
531 throughout the study region. In reference to Figure 9, each system parameter, with the exception  
532 of litter pool decomposition, is the most influential in controlling NO<sub>3</sub> fate and transport in at  
533 least several areas within the study region. N fertilizer loading is the dominant parameter in the  
534 majority of cultivated areas, although N uptake, heterotrophic denitrification, and NO<sub>3</sub>  
535 concentration in canal water also are the most influential in much of the study area. The rate of  
536 autotrophic denitrification ( $\lambda_{NO_3}^{auto}$ ) is influential in many of the areas adjacent to outcropped  
537 marine shale. However, it is interesting to note that there are many locations in the study area  
538 adjacent to outcropped shale in which  $\lambda_{NO_3}^{auto}$  is not the dominant parameter. These locations are  
539 indicated by circles in Figure 9F. In these areas, other system inputs and processes are dominant,  
540 demonstrating that knowledge of shale locations alone cannot be used to determine where  
541 groundwater NO<sub>3</sub> concentration will be affected the most by autotrophic denitrification.

542 Whereas other studies [Chaplot et al., 2004; Botter et al., 2006; Wriedt and Rode, 2006; Almasri  
543 and Kaluarachchi, 2007; Arabi et al., 2007; Schilling et al., 2007; Bailey et al., 2015] have  
544 focused on the response of the entire groundwater and/or watershed system, the novelty of this  
545 study is the assessment of NO<sub>3</sub> transport control in localized areas within a region. Almasri and  
546 Kaluarachchi [2007] stated that the importance of denitrification in controlling NO<sub>3</sub> in  
547 groundwater may differ from location to location. In this study we quantify this difference  
548 spatially for denitrification and for each of the other eight targeted parameters (see Figure 9).

549

## 550 **5 Summary and Concluding Remarks**

551 This study used a 506 km<sup>2</sup> regional-scale N fate and transport numerical model to examine the  
552 influence of forcing terms (fertilizer loading, crop N uptake, N concentration of applied  
553 irrigation water and canal seepage  $Canal_{NO_3}$ ) and chemical processes (litter and humus organic N  
554 decomposition; nitrification of NH<sub>4</sub> to NO<sub>3</sub>; heterotrophic and autotrophic reduction of NO<sub>3</sub>,  
555 with the latter occurring in the presence of pyrite-bearing marine shale; and autotrophic  
556 reduction of O<sub>2</sub>, also occurring in the presence of shale) on NO<sub>3</sub> concentration in groundwater  
557  $C_{NO_3}$ , NO<sub>3</sub> leaching from the unsaturated zone to the saturated zone of the aquifer, and NO<sub>3</sub> mass  
558 loading from the aquifer to the Arkansas River via groundwater discharge. The influence of each  
559 of the 9 model factors was computed using the revised Morris method for sensitivity analysis,  
560 with results processed to determine parameter influence globally for the entire study region and  
561 specific to crop type, canal command area (i.e. the group of fields receiving irrigation water from  
562 a given canal), and individual grid cells. For the latter, spatial plots of sensitivity indices are  
563 presented to display the spatial distribution of influence for each model factor.

564 Results indicate that, generally, fertilizer loading, crop N uptake, and heterotrophic  
565 denitrification governed NO<sub>3</sub> mass transport, particularly in cultivated areas. However, their  
566 order of influence on  $C_{NO_3}$  and NO<sub>3</sub> mass leaching varies according to crop type and command  
567 area, and several command areas are influenced more, or at least to a significant degree, by  
568 nitrification, autotrophic denitrification, and  $Canal_{NO_3}$ . Spatial plots of cell-by-cell sensitivity

569 indices enhance further the understanding of localized model factor influence, with each factor  
570 except for rate of heterotrophic O<sub>2</sub> reduction having the dominant influence over  $C_{NO_3}$  at one or  
571 more locations within the study area. Results also indicate that the concentration of O<sub>2</sub> in  
572 groundwater  $C_{O_2}$  is governed by rates of organic matter decomposition, which releases CO<sub>2</sub> and  
573 hence enhances heterotrophic reduction of O<sub>2</sub>.

574 In general, the procedure followed in this study provides key information regarding overall NO<sub>3</sub>  
575 fate and transport in an agricultural groundwater system, guidance for future data collection and  
576 monitoring programs, an indication of which parameters should be targeted during model  
577 parameter estimation, and guidance for implementing best-management practices (BMPs) for  
578 NO<sub>3</sub> remediation, i.e. decreasing groundwater concentrations and mass loading to the stream  
579 network. For example, fertilizer loading, crop N uptake, and  $Canal_{NO_3}$  should be targeted in field  
580 data collection and observation, with  $Canal_{NO_3}$  monitored for each irrigation canal as often as  
581 possible, whereas first-order kinetic rate constants for nitrification, denitrification, and organic  
582 matter decomposition should be targeted during parameter estimation efforts. Furthermore, the  
583 procedure followed in this study also allows for data collection, management practice  
584 implementation, and parameter estimation to be performed on location-specific basis. For  
585 example, results suggest that a specific BMP (e.g., reduction in N fertilizer loading) may be  
586 optimal for several of the command areas but not for others, or that decreasing  $Canal_{NO_3}$  or the  
587 amount of NO<sub>3</sub> denitrified in shale outcrop locations will help remediate NO<sub>3</sub> only in a few  
588 specific locations within the study area. Also, data collecting points for specific model factors  
589 can be restricted to sub-region areas, either to a given command area or, with the use of the  
590 spatial plots of sensitivity indices, to even more localized sites.

591

592

593 **Acknowledgements**

594 Financial support for this study was provided by grants from the Colorado Department of Public  
595 Health and Environment (03-00837, 05-00112, 05-00170, 09-00169, PO FAA WQC1349262),

596 the Colorado Agricultural Experiment Station (COL00684), and the United States Bureau of  
597 Reclamation (99-FC-60-12140). The cooperation of numerous landowners in the LARV in  
598 providing access for field monitoring is greatly appreciated. The views and conclusions  
599 contained in this document are those of the authors and should not be interpreted as representing  
600 the opinions or policies of the government of Colorado or the U.S. government. Data used in this  
601 study can be provided via a request to the corresponding author at rtbailey@engr.colostate.edu.  
602 The authors thank Colorado State University Libraries' support for publication costs. The  
603 authors thank two anonymous reviewers for their thorough and helpful reviews to improve the  
604 content of this paper.

605

606

607 **References**

608 Almasri, M.N., and J.J. Kaluarachchi (2007), Modeling nitrate contamination of groundwater in  
609 agricultural watersheds. *J. Hydrol.* 343: 211-229.

610 Arabi, M., R.S. Govindaraju, B. Engel, and M. Hantush (2007), Multiobjective sensitivity  
611 analysis of sediment and nitrogen processes with a watershed model. *Water Resources Research*  
612 43, W06409, doi:10.1029/2006WR005463.

613 Bailey, R.T., W.J. Hunter, and T.K. Gates (2012), The influence of nitrate on selenium in  
614 irrigated agricultural groundwater systems. *J. Environ. Qual.* 41(3): 783-792.

615 Bailey, R.T., E.D. Morway, R. Niswonger, and T.K. Gates (2013a), Modeling variably saturated  
616 multispecies reactive groundwater solute transport with MODFLOW-UZF and RT3D.  
617 *Groundwater* 51(5): 752-761.

618 Bailey, R.T., T.K. Gates, and A.D. Halvorson (2013b), Simulating variably-saturated reactive  
619 transport of selenium and nitrogen in agricultural groundwater systems. *J. Contam. Hydrol.* 149:  
620 27-45.

621 Bailey, R.T., T.K. Gates, and M. Ahmadi (2014), Simulating reactive transport of selenium  
622 coupled with nitrogen in a regional-scale irrigated groundwater system. *J. Hydrol.* 515: 29-46.

*Environmental Factors Governing NO<sub>3</sub> Transport*

- 623 Bailey, R.T. and M. Ahmadi (2014), Spatial and temporal variability of in-stream water quality  
624 parameter influence on dissolved oxygen and nitrate within a regional stream network.  
625 Ecological Modelling 277, 87-96. doi: 10.1016/j.ecolmodel.2014.01.015.
- 626 Bailey, R.T., Gates, T.K., and E.C. Romero (2015), Assessing the effectiveness of land and  
627 water management practices on nonpoint source nitrate levels in an alluvial stream-aquifer  
628 system. J. Cont. Hydrology 179, 102-115.
- 629 Birkinshaw, S.J., and J. Ewen (2000), Nitrogen transformation component for SHETRAN  
630 catchment nitrate transport modelling. J. Hydrol. 230: 1-17.
- 631 Botter, G., Settin, T., Marani, M., and A. Rinaldo (2006), A stochastic model of nitrate transport  
632 and cycling at basin scale. Water Res. Research 42, doi: 10.1029/2005WR004599.
- 633 Cacuci, D. G. (2003), Sensitivity and Uncertainty Analysis, Volume I: Theory, CRC Press, Boca  
634 Raton, Florida.
- 635 Campolongo, F. and A. Saltelli (1997), Sensitivity analysis of an environmental model: an  
636 application of different analysis methods. Reliability Engineering & System Safety 57(1), 49–69,  
637 doi: 10.1016/S0951-8320(97)00021-5.
- 638 Campolongo, F. and R. Braddock, R. (1999), Sensitivity analysis of the IMAGE Greenhouse  
639 model. Environmental Modelling & Software 14(4), 275–282, doi: 10.1016/S1364-  
640 8152(98)00079-6.
- 641 Campolongo, F., J. Cariboni, and A. Saltelli (2007), An effective screening design for sensitivity  
642 analysis of large models, Environmental Modelling & Software 22(10), 1509–1518,  
643 doi:10.1016/j.envsoft.2006.10.004.
- 644 Colorado Department of Public Health and Environment (CDPHE). 2012. “Regulation No. 31:  
645 The Basic Standards and Methodologies for Surface Water.” Denver, Colorado.

*Environmental Factors Governing NO<sub>3</sub> Transport*

- 646 Chaplot, V., A. Saleh, D.B. Jaynes, and J. Arnold (2004), Predicting water, sediment and NO<sub>3</sub>-N  
647 loads under scenarios of land-use and management practices in a flat watershed., Water, Air, and  
648 Soil Pollution 154: 271-293.
- 649 Conan, E., F. Bouraoui, N. Turpin, G. de Marsily, and G. Bidoglio (2003), Modeling flow and  
650 nitrate fate at catchment scale in Brittany (France). J. Environ. Qual., 32: 2026-2032.
- 651 Cox, B.A., and P.G. Whitehead (2005), Parameter sensitivity and predictive uncertainty in a new  
652 water quality model, Q<sup>2</sup>. J. Environ. Engr. 131, 147-157.
- 653 Cukier, R., Fortuin, C.M., Schuler, K.E., Petschek, A.G., and J.H. Schaibly (1973), Study of the  
654 sensitivity of coupled reaction systems to uncertainties in rate coefficients. i theory. J. Chem.  
655 Physics 59, 3873-3878.
- 656 Deflandre, A., R.J. Williams, F.J. Elorza, J. Mira, and D.B. Doorman (2006), Analysis of the  
657 QUESTOR water quality model using a Fourier amplitude sensitivity test (FAST) for two UK  
658 rivers. Science of the Total Environ. 360, 290-304.
- 659 Ehteshami, M., A.S. Langeroudi, and S. Tavassoli (2013), Simulation of nitrate contamination in  
660 groundwater caused by livestock industry (cast study: Rey). J. Environ. Protection 4, 91-97.
- 661 Fan, A.M., and V.E. Steinberg (1996), Health implications of nitrate and nitrite in drinking  
662 water: an update on methemoglobinemia occurrence and reproductive and developmental  
663 toxicity. Regulatory Toxicology and Pharmacology 23, 35-43.
- 664 Frind, E.O., W.H.M. Duynisveld, O. Strelbel, J. Boettcher (1990), Modeling of multicomponent  
665 transport with microbial transformation in groundwater: the Fuhrberg case. Water Resour. Res.  
666 26 (8), 1707–1719.
- 667 Gates, T.K., B.M. Cody, J.P. Donnelly, A.W. Herting, R.T. Bailey, and J. Mueller-Price (2009),  
668 Assessing Selenium contamination in the irrigated stream-aquifer system of the Arkansas River,  
669 Colorado. J. Environ. Qual., 38: 2344-2356.

*Environmental Factors Governing NO<sub>3</sub> Transport*

- 670 Hall J.W., Tarantola S., Bates P.D., and M.S. Horritt (2005), Distributed sensitivity analysis of  
671 flood inundation model calibration. *J. Hydraul. Eng.* 131:117 – 26.
- 672 Hall, J. W., S. A. Boyce, Y. Wang, R. J. Dawson, S. Tarantola, and A. Saltelli (2009), Sensitivity  
673 analysis for hydraulic models, *J. Hydraul. Eng.*, 135(11), 959, doi:10.1061/(ASCE)HY.1943-  
674 7900.0000098.
- 675 Hartmann, A., Weiler, M., Wagener, T., Lange, J., Kralik, M., Humer, F., Mizyed, N., Rimmer,  
676 A., Barberá, J. A., Andreo, B., Butscher, C. and P. Huggenberger (2013), Process-based karst  
677 modelling to relate hydrodynamic and hydrochemical characteristics to system properties.  
678 *Hydrol. Earth Syst. Sci.*, 17(8), 3305–3321, doi:10.5194/hess-17-3305-2013.
- 679 Hefting, M.M., and J.J.M. de Klein (1998), Nitrogen removal in buffer strips along a lowland  
680 stream in the Netherlands: a pilot study. *Environ. Pollut.*, 102, 521–526.
- 681 Holloway, J. M., and R. A. Dahlgren. (2002). Nitrogen in rock: Occurrences and  
682 biogeochemical implications. *Global Biogeochem. Cycles*, 16(4), 65-1 – 65-17.
- 683 Iman, R.L. and W.J. Conover (1987), A measure of top-down correlation. *Technometrics*  
684 293, 351-357.
- 685 Johnsson, H., L. Bergström, P. Jansson, and K. Paustian (1987), Simulated nitrogen dynamics  
686 and losses in a layered agricultural soil. *Agric. Ecosyst. Environ.* 18: 333-356.
- 687 Jørgensen, C.J., O.S. Jacobsen, B. Elberling, and J. Aamand (2009), Microbial oxidation of  
688 pyrite coupled to nitrate reduction in anoxic groundwater sediment. *Environ. Sci. Technol.* 43,  
689 4851-4857.
- 690 Kelleher, C., Wagener, T., McGlynn, B., Ward, A. S., Gooseff, M. N. and R. A. Payn (2013),  
691 Identifiability of transient storage model parameters along a mountain stream, *Water Resour.*  
692 *Res.*, doi:10.1002/wrcr.20413.
- 693 Korom, S.F. (1992), Natural denitrification in the saturation zone: a review. *Water Resour. Res.*  
694 28 (6), 1657–1668.

*Environmental Factors Governing NO<sub>3</sub> Transport*

- 695 Lee, M., G. Park, M. Park, J. Park, J. Lee, and S. Kim (2010), Evaluation of non-point source  
696 pollution reduction by applying best management practices using a SWAT model and QuickBird  
697 high resolution satellite imagery. *J. Environmental Sciences* 22(6): 826-833.
- 698 Liu, D., and Z. Zou (2012), Sensitivity analysis of parameters in water quality models and water  
699 environment management. *J. Environmental Protection* 3, 863-870.
- 700 Ma, L., M. J. Shaffer, J. K. Boyd, R. Waskom, L. R. Ahuja, K. W. Rojas, and C. Xu (1998),  
701 Manure Management in an Irrigated Silage Corn Field: Experiment and Modeling. *Soil Sci. Soc.*  
702 *Am. J.* 62:1006-1017.
- 703 McNab Jr., W.W., and B.P. Dooher (1998), Uncertainty analysis of fuel hydrocarbon  
704 biodegradation signatures in groundwater by probabilistic modeling. *Ground Water* 36 (4), 69–  
705 698.
- 706 Molénat, J. and C. Gascuel-Odoux (2002), Modelling flow and nitrate transport in groundwater  
707 for the prediction of water travel times and of consequences of land use evolution on water  
708 quality. *Hydrological Processes* 16, 479-492.
- 709 Montross, G. G., B. L. McGlynn, S. N. Montross, and K. K. Gardner (2013), Nitrogen  
710 production from geochemical weathering of rocks in southwest Montana, USA. *J. Geophys.*  
711 *Res.: Biosci.*, 118, 1068-1078.
- 712 Morris, M., 1991. Factorial sampling plans for preliminary computational experiments.  
713 *Technometrics* 33(2), 161–174.
- 714 Morway, E. D., and T.K. Gates (2012), Regional assessment of soil water salinity across an  
715 intensively irrigated river valley. *J. Irrig. Drain. Engrg.*, 138(5): 393-405.
- 716 Morway, E. D., T.K. Gates, and R.G. Niswonger (2013), Appraising options to enhance shallow  
717 groundwater table and flow conditions over regional scales in an irrigated alluvial aquifer  
718 system. *J. Hydrol.*, 495: 216-237.

*Environmental Factors Governing NO<sub>3</sub> Transport*

- 719 Niswonger, R.G., D.E. Prudic, and R.S. Regan (2006), Documentation of the unsaturated-zone  
720 flow (UZF1) package for modeling unsaturated flow between the land surface and the water  
721 table with MODFLOW-2005, U.S. Geological Survey Techniques and Methods 6-A19.
- 722 Niswonger, R.G., S. Panday, and I. Motomu (2011), MODFLOW-NWT, A Newton formulation  
723 for MODFLOW-2005: U.S. Geological Survey Techniques and Methods 6-A37: 44 p.
- 724 Ocampo, C.J., M. Sivapalan, and C.E. Oldham (2006), Field exploration of coupled hydrological  
725 and biogeochemical catchment responses and a unifying perceptual model. *Adv. Water Resour.*,  
726 29, 161-180.
- 727 Oyarzun, R., J. Arumí, L. Salgado, and M. Mariño (2007), Sensitivity analysis and field testing  
728 of the RISK-N model in the Central Valley of Chile. *Agricul. Water Management* 87, 251-260.
- 729 Parkin, T.B. and J.A. Robinson (1989), Stochastic models of soil denitrification. *Appl. Environ.*  
730 *Micro.* 55 (1), 72–77.
- 731 Reusser, D.E., W. Buytaert, and E. Zehe (2011), Temporal dynamics of model parameters  
732 sensitivity for computationally expensive models with the Fourier amplitude sensitivity test.  
733 *Water Resources Research* 47, W07551,doi:10.1029/2010WR009947.
- 734 Rong, Y., and W. Xuefeng (2011), Effects of nitrogen fertilizer and irrigation rate on nitrate  
735 present in the profile of a sandy farmland in Northwest China. *Procedia Environ. Sci.* 11: 726-  
736 732.
- 737 Sahu, M., and R.R. Gu (2009), Modeling the effects of riparian buffer zone and contour strips on  
738 stream water quality, *Ecol. Engr.* 35: 1167-1177.
- 739 Saltelli, A., M. Ratto, T. Andres, F. Campolongo, J. Cariboni, D. Gatelli, M. Saisana, and S.  
740 Tarantola (2008), *Global Sensitivity Analysis. The Primer*, John Wiley and Sons. West Sussex,  
741 England.

*Environmental Factors Governing NO<sub>3</sub> Transport*

- 742 Schilling, K.E., Tomer, M.D., Zhang, Y.-K., Weisbrod, T., and P. Jacobson (2007),  
743 Hydrogeologic controls on nitrate transport in a small agricultural catchment, Iowa. J. Geoph.  
744 Researrch 112, doi:10.1029/2007JG000405.
- 745 Scott, G. R. (1968), Geologic and structure contour map of the La Junta quadrangle, Colorado  
746 and Kansas, edited by U. S. G. Survey, Reston, Virginia.
- 747 Sharps, J. A. (1976), Geologic map of the Lamar quadrangle, Colorado and Kansas, edited by U.  
748 S. G. Survey, Reston, Virginia.
- 749 Sincock, A.M., H.S. Wheater, and P.G. Whitehead (2003), Calibration and sensitivity analysis of  
750 a river water quality model under unsteady flow conditions. J. Hydrology 227, 214-229.
- 751 Sobol', I.M. (1993), Sensitivity analysis for non-linear mathematical models. Mathematical  
752 Modelling and Computational Experiment 1, 407-414.
- 753 Spalding, R.F., and M.E. Exner (1993), Occurrence of nitrate in groundwater: A review. J.  
754 Environ. Qual. 22, 392-402.
- 755 Spruill, T.B. (2000), Statistical evaluation of effects of riparian buffers on nitrate and ground  
756 water quality, J. Environ. Qual. 29: 1523-1538.
- 757 Sun, X., L. Newham, B. Croke, and J. Norton (2012), Three complementary methods for  
758 sensitivity analysis of a water quality model. Environmental Modelling & Software 37, 19–29,  
759 doi: 10.1016/j.envsoft.2012.04.010.
- 760 Vaché, K.B., J.M. Eilers, and M.V. Santelmann (2002), Water quality modeling of alternative  
761 agricultural scenarios in the U.S. Corn Belt, J. Amer. Water Resour. Assoc. 38(3): 773-787.
- 762 White, K. L., and I. Chaubey (2005), Sensitivity analysis, calibration, and validations for a  
763 multisite and multivariable SWAT model, J. Am. Water Resour. Association, 41(5), 1077–1089,  
764 doi:10.1111/j.1752-1688.2005.tb03786.x.

*Environmental Factors Governing NO<sub>3</sub> Transport*

- 765 Wriedt, G., and M. Rode (2006), Modelling nitrate transport and turnover in a lowland  
 766 catchment system. *J. Hydrol.*, 328, 157-176.
- 767 Wu, W.-M., J. Carley, S.J. Green, J. Luo, S.D. Kelly, J.V. Nostrand, K. Lower, T. Mehlhorn, S.  
 768 Carroll, B. Boonchayananant, F.E. Löfller, D. Watson, K.M. Kemner, J. Zhou, P.K. Kitanidis, J.E.  
 769 Kostka, P.M. Jardine, and C.S. Criddle (2010), Effects of nitrate on the stability of uranium in a  
 770 bioreduced region of the subsurface. *Environ. Sci. Techno.*, 44, 5104-5111.
- 771 Zielinski, R. A., S. Asher-Bolinder, A. L. Meier, C. A. Johnson, and B. J. Szabo. (1997). Natural  
 772 or fertilizer-derived uranium in irrigation drainage: a case study in southeastern Colorado, USA.  
 773 *Appl. Geochem.*, 12, 9 – 21.
- 774
- 775
- 776
- 777
- 778 Table 1. Baseline agricultural management and crop parameter values for the model simulations.

Crop Type	Planting Day	Harvest Day	Plow Day	$P_{St}$	$d_{rt,max}$	$CN_{RT}$	$F_{NH_4}$	$N_{up}$
Units	-	-	-	kg ha <sup>-1</sup>	m	-	kg ha <sup>-1</sup>	kg ha <sup>-1</sup>
Alfalfa	30-Apr	30-Sep	20-Oct	561.6	1.83	25	22.4	22.4
Bean	20-May	30-Sep	20-Oct	561.6	0.91	25	140	84.2
Corn	1-May	25-Oct	14-Nov	5616	1.22	70	252	224.6
Melon	15-May	10-Aug	30-Aug	561.6	1.22	25	112	112.3
Onion	20-Mar	15-Sep	5-Oct	561.6	0.46	25	140	78.6
Pasture	30-Aug	30-Sep	20-Oct	0	0.91	70	140	112.3
Pumpkin	1-Jun	30-Sep	20-Oct	561.6	0.91	25	140	84.2
Sorghum	20-May	15-Oct	4-Nov	1684.8	0.91	70	112	112.3
Spring Grain	1-Apr	15-Jul	4-Aug	1684.8	0.91	70	112	112.3
Squash	20-May	25-Jul	14-Aug	561.6	0.91	25	140	84.2
Sunflower	1-Jun	10-Oct	30-Oct	561.6	0.91	25	140	84.2
Vegetable	25-Apr	30-Aug	19-Sep	561.6	0.91	25	140	84.2
Winter Wheat	30-Sep	5-Jul	25-Jul	1684.8	0.91	70	112	112.3

779  $d_{pw}$  (depth of plowing) is 1.0 m for all crops except beans (0.8 m)

780  $P_{Rt}$  (seasonal mass of root mass) is 500 kg ha<sup>-1</sup> for all crop types

781  $CN_{ST}$  (carbon:nitrogen ratio in stover mass) is 50 for all crop types

782

*Environmental Factors Governing NO<sub>3</sub> Transport*

783 Table 2. Parameters and values for chemical reactions involving organic matter decomposition, dissolved oxygen,  
 784 and nitrogen species for the baseline simulation model.

Org. Matter Decomp.			Dissolved Oxygen			Nitrogen		
Param.	Value	Unit	Param.	Value	Unit	Param.	Value	Unit
$\lambda_L$	0.25	d <sup>-1</sup>	$\lambda_{O_2}^{het}$	2.0	d <sup>-1</sup>	$H_{C/N}$	12.0	-
$\lambda_H$	0.003	d <sup>-1</sup>	$\lambda_{O_2}^{auto *}$	0.58	d <sup>-1</sup>	$B_{C/N}$	8.0	-
$f_e$	0.5	-	$K_{O_2}$	1.0	g m <sup>-3</sup>	$I_{O_2}$	1.0	g m <sup>-3</sup>
$f_h$	0.2	-				$\lambda_{nit}^*$	0.98	d <sup>-1</sup>
$K_{CO_2}$	0.75	g m <sup>-3</sup>				$\lambda_{vol}$	0.1	d <sup>-1</sup>
						$\lambda_{NO_3}^{het}$	0.1	d <sup>-1</sup>
						$\lambda_{NO_3}^{auto *}$	0.22	d <sup>-1</sup>
						$K_{NO_3}$	10.0	g m <sup>-3</sup>
						$K_{d,NH_4}$	3.5	-

785 \* Indicates mean value, with specific values assigned to each command area according to the values reported in Bailey et al. (2014).

786

787

788

789

790

791

792

793

794

795

796

797

798

799

800

801

802

*Environmental Factors Governing NO<sub>3</sub> Transport*

803 Table 3. Sensitivity index ( $\mu^*$ ) for each of the model input factors investigated, indicating the degree of parameter  
 804 influence on  $C_{NO_3}$  in the shallow saturated zone of the aquifer (in layer 4 of the grid) for the grid cells associated with  
 805 each crop type and command area, with the values of the top three influential parameters for each crop type and  
 806 command area bolded.

	N Fert. Loading	N uptake	Litter decomp.	Humus decomp.	O <sub>2</sub> reduction	Nitrif.	Het. Denitrif.	Auto. Denitrif.	NO <sub>3</sub> canal conc.
	$F_{NH_4}$	$N_{up}$	$\lambda_L$	$\lambda_H$	$\lambda_{O_2}^{auto}$	$\lambda_{nit}$	$\lambda_{NO_3}^{het}$	$\lambda_{NO_3}^{auto}$	$Canal_{NO_3}$
<b>Crop</b>									
Alfalfa	<b>0.46</b>	<b>0.56</b>	0.03	0.09	0.00	0.06	<b>0.23</b>	0.04	0.11
Bean	<b>0.70</b>	<b>0.43</b>	0.04	0.09	0.00	0.03	<b>0.34</b>	0.00	0.06
Corn	<b>0.94</b>	<b>0.72</b>	0.04	0.10	0.00	0.03	<b>0.30</b>	0.03	0.09
Melon	<b>5.46</b>	<b>3.02</b>	0.10	0.15	0.00	0.23	<b>0.92</b>	0.00	0.47
Onion	<b>1.21</b>	<b>0.99</b>	0.02	0.14	0.00	0.03	0.19	0.01	<b>0.45</b>
Pasture	<b>0.66</b>	<b>0.63</b>	0.03	0.12	0.01	0.04	<b>0.32</b>	0.07	0.14
Sorghum	<b>0.84</b>	<b>0.81</b>	0.03	0.12	0.00	0.08	<b>0.28</b>	0.04	0.13
Spring Grain	<b>0.79</b>	<b>0.70</b>	0.04	0.13	0.00	0.02	<b>0.32</b>	0.02	0.06
<b>Command Area</b>									
Catlin	<b>0.12</b>	<b>0.26</b>	0.00	0.03	0.01	<b>0.16</b>	0.04	0.01	0.11
Fort Lyon	<b>0.92</b>	<b>0.81</b>	0.05	0.17	0.00	0.04	<b>0.42</b>	0.08	0.12
Highline	<b>0.69</b>	<b>0.51</b>	0.03	0.06	0.00	0.02	0.23	0.01	<b>0.26</b>
Holbrook	<b>0.28</b>	<b>0.29</b>	0.02	0.03	0.00	0.01	0.08	<b>0.11</b>	0.10
Otero	<b>1.21</b>	<b>1.16</b>	0.05	0.14	0.00	0.04	0.49	0.04	<b>0.59</b>
RF Ditch	0.14	<b>0.15</b>	0.01	0.03	0.02	0.01	0.14	<b>0.20</b>	<b>0.51</b>

807

808

809

810

811

812

813

814

815

816

817

818

819

820

*Environmental Factors Governing NO<sub>3</sub> Transport*

821 Table 4. Sensitivity index ( $\mu^*$ ) for each of the model input factors investigated, indicating the degree of parameter  
 822 influence on NO<sub>3</sub> mass leaching from the shallow soil zone for the grid cells associated with each crop type and  
 823 command area, , with the values of the top three influential parameters for each crop type and command area bolded.

	N Fert. Loading	N uptake	Litter decomp.	Humus decomp.	O <sub>2</sub> reduction	Nitrif.	Het. Denitrif.	Auto. Denitrif.	NO <sub>3</sub> canal conc.
	$F_{NH_4}$	$N_{up}$	$\lambda_L$	$\lambda_H$	$\lambda_{O_2}^{auto}$	$\lambda_{nit}$	$\lambda_{NO_3}^{het}$	$\lambda_{NO_3}^{auto}$	$Canal_{NO_3}$
<b>Crop Type</b>									
Alfalfa	<b>396</b>	<b>614</b>	19	73	0.8	39	<b>176</b>	13	108
Bean	<b>43</b>	<b>26</b>	2.7	7.6	0.0	2.3	<b>22</b>	0.0	3.6
Corn	<b>486</b>	<b>367</b>	26	51	0.2	15	<b>172</b>	1.0	41
Melon	<b>7.0</b>	<b>4.5</b>	0.2	0.2	0.0	0.2	<b>1.9</b>	0.0	0.6
Onion	<b>9.7</b>	<b>7.2</b>	0.2	0.4	0.0	0.4	1.1	0.0	<b>1.6</b>
Pasture	<b>431</b>	<b>382</b>	16	76	0.4	9.0	<b>162</b>	12	49
Sorghum	<b>271</b>	<b>221</b>	11	29	0.1	11	<b>94</b>	2.1	26
Spring Grain	<b>213</b>	<b>179</b>	11	31	0.2	2.9	<b>82</b>	1.3	14
<b>Command Area</b>									
Catlin	<b>35</b>	<b>63</b>	0.9	5.3	0.1	<b>38</b>	7.5	0.3	9.2
Fort Lyon	<b>852</b>	<b>777</b>	35	140	1.0	33	<b>335</b>	13	70
Highline	<b>125</b>	<b>103</b>	4.2	12	0.0	2.7	<b>41</b>	0.1	37
Holbrook	<b>70</b>	<b>71</b>	3.6	5.7	0.1	2.6	<b>21</b>	3.6	10
Otero	<b>196</b>	<b>176</b>	8.4	21	0.0	4.7	<b>85</b>	2.0	62
RF Ditch	<b>3.6</b>	<b>3.9</b>	0.1	1.2	0.2	0.5	1.9	3.3	<b>30</b>

824

825

826

827

828

829

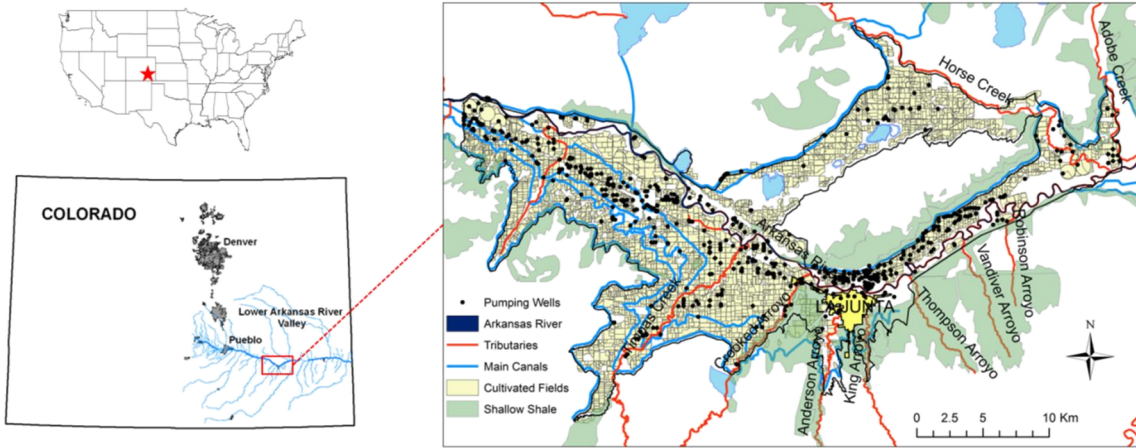
830

831

832

833

*Environmental Factors Governing NO<sub>3</sub> Transport*



834  
835 Figure 1. Location and hydrologic features of the study region in the Lower Arkansas River Valley in southeastern  
836 Colorado, showing the Arkansas River and tributaries (red), cultivated fields (yellow), irrigation canals (light blue),  
837 groundwater pumping wells (black dots), and the extent of near-surface shale (within 2 m of the ground surface)  
838 (green).

839

840

841

842

843

844

845

846

847

848

849

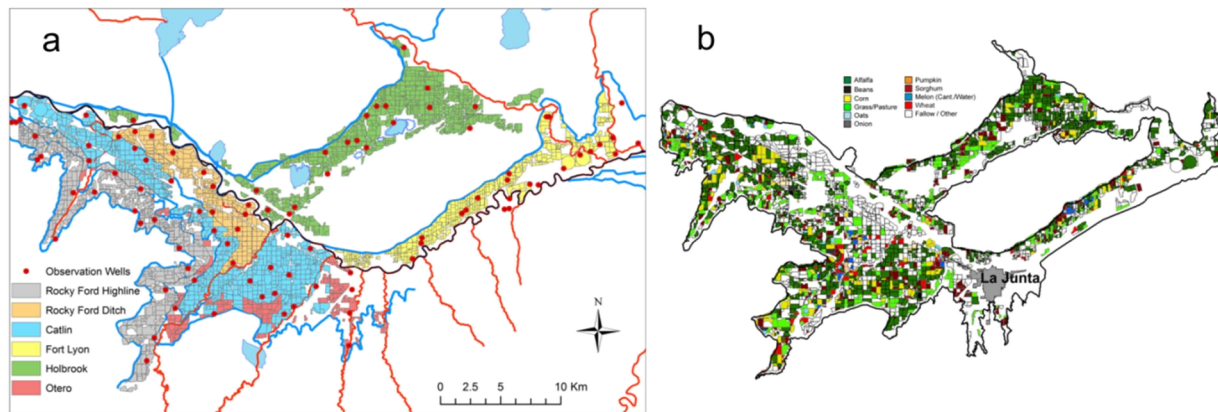
850

851

852

853

*Environmental Factors Governing NO<sub>3</sub> Transport*



854

855 Figure 2. Features of the cultivation and data collection of the study region, including (a) canal command areas and  
856 location of groundwater observation wells, with a command area defined as the collection of fields receiving  
857 irrigation water from the same canal, and (b) the spatial distribution of crop cultivation during the 2006 growing  
858 season.

859

860

861

862

863

864

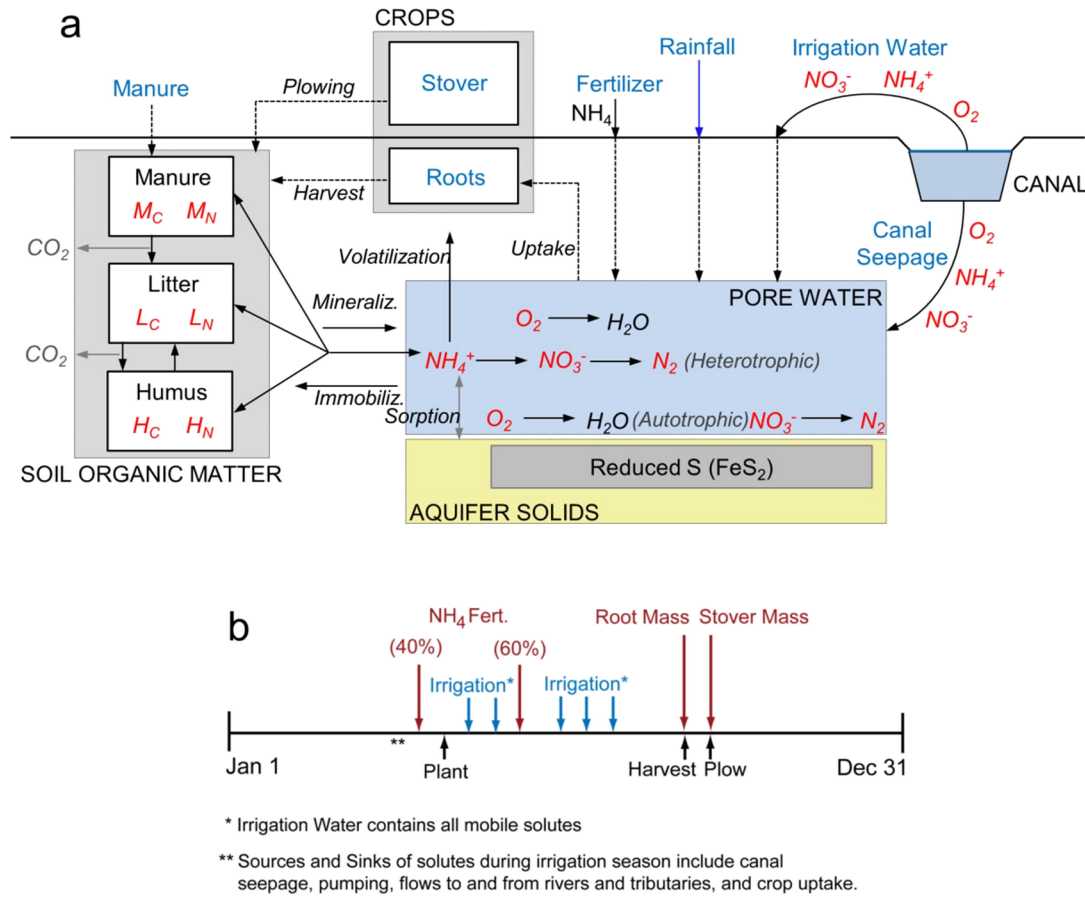
865

866

867

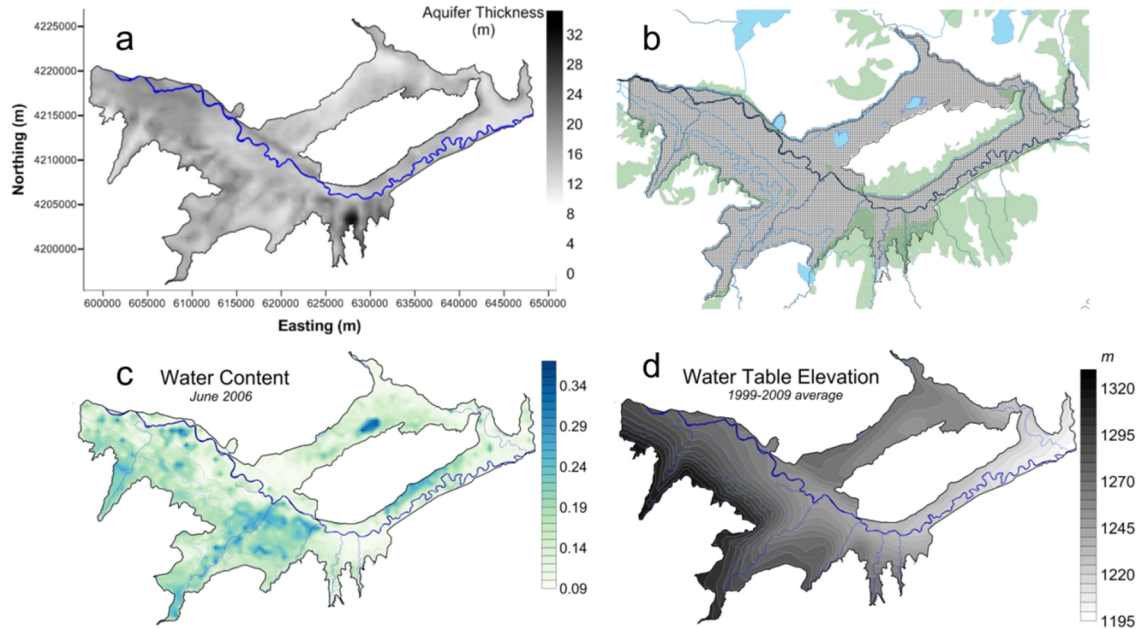
868

869



870

871 Figure 3. Depiction of the main processes simulated by the N reaction module of the UZF-RT3D model, with (a) conceptual model of the fate and transport of  $\text{O}_2$  and N species in an irrigated soil-aquifer system wherein fertilizer,  
872 irrigation, and canal seepage bring solute mass into the subsurface environment, and (b) the annual cultivation  
873 schedule used in the N reaction module, including timing of planting, fertilizer loading, irrigation application,  
874 harvest, and plowing.  $\text{NH}_4$  fertilizer has a split loading, with 40% of the loading occurring 2 weeks before planting,  
875 and the remainder applied 6 weeks after planting.



877

878 Figure 4. (a) The spatial distribution of aquifer thickness (m) of the alluvium in the study region, (b) the finite-  
879 difference grid used in the calibrated and tested MODFLOW-UZF1 groundwater flow model, using 250 m by 250 m  
880 grid cells, (c) spatial distribution of soil water content simulated by the MODFLOW-UZF1 model, for June 2006,  
881 and (d) average-simulated water table elevation for the 1999-2009 time period.

882

883

884

885

886

887

888

889

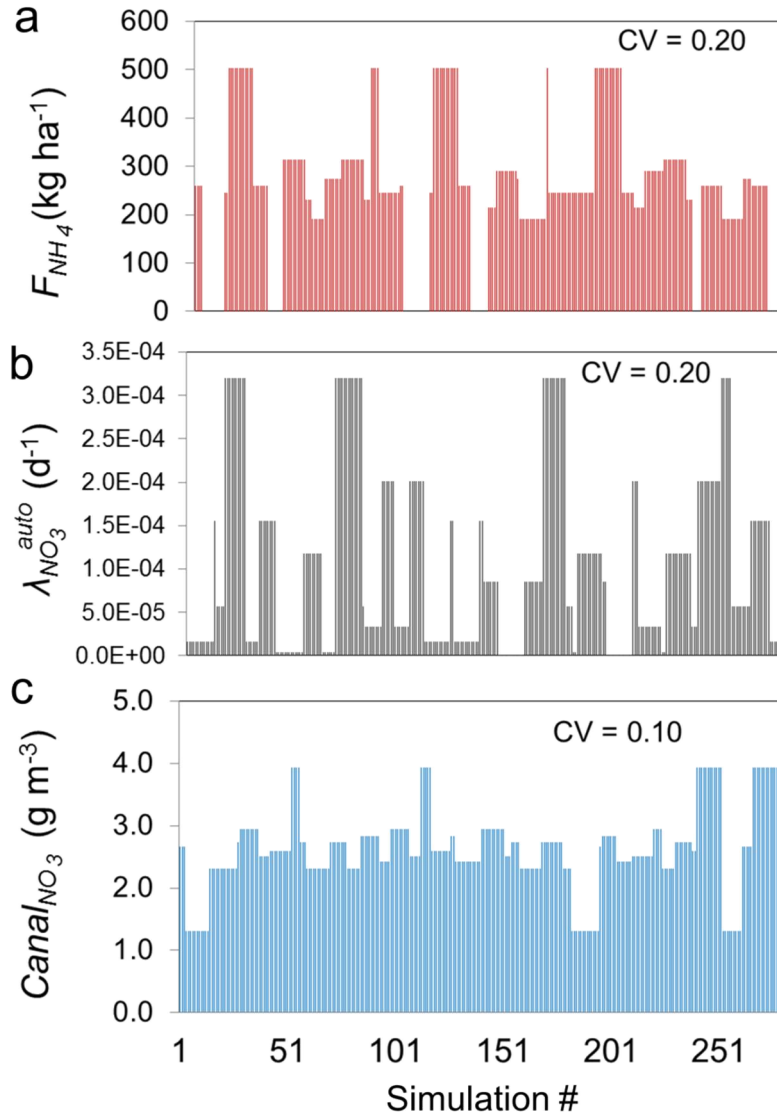
890

891

892

893

894



895

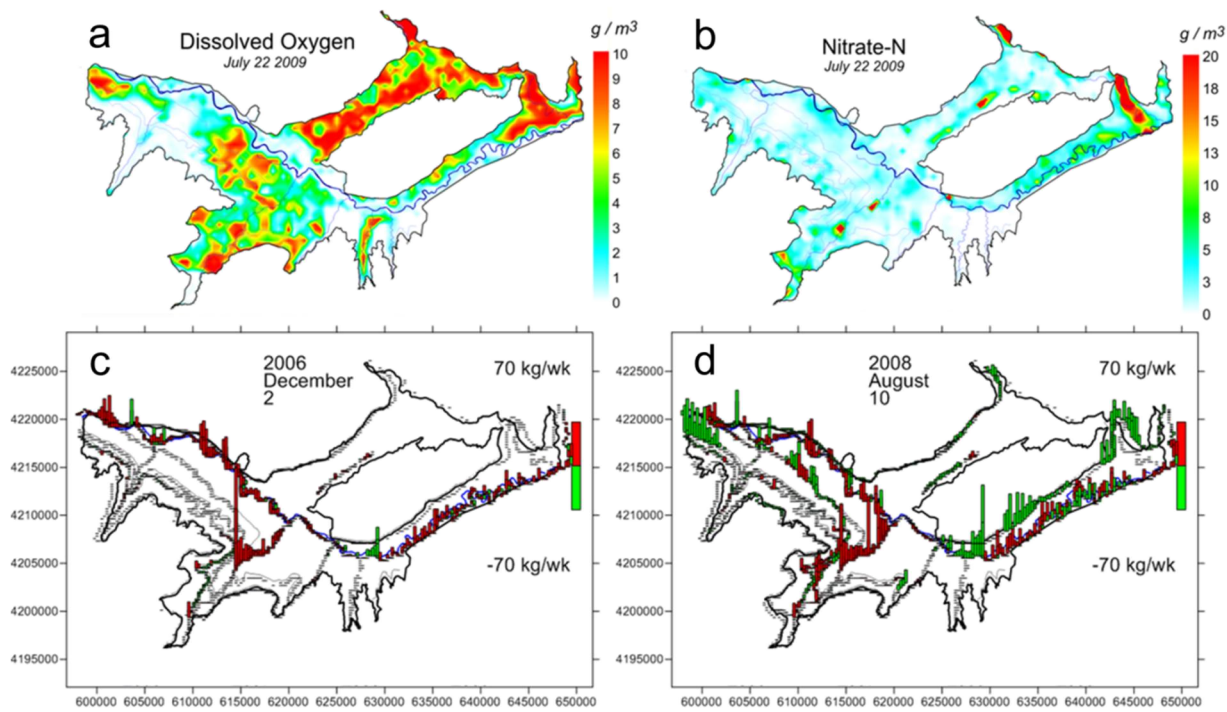
896 Figure 5. Values of (a) fertilizer loading  $F_{NH_4}$  (kg/ha) for corn, and (b) first-order rate constant of autotrophic  
 897 denitrification  $\lambda_{NO_3}^{auto}$  (1/day) and (c) nitrate concentration of canal water  $Canal_{NO_3}$  (mg/L) for the Rocky Ford Highline  
 898 canal command area, for each of the 280 simulations in the revised Morris SA scheme.

899

900

901

Environmental Factors Governing  $NO_3$  Transport



902

903 Figure 6. Summary of typical UZF-RT3D model results for the study region, showing spatial distribution of (a)  $C_{O_2}$   
904 and (b)  $C_{NO_3}$  in shallow groundwater, and spatial distribution of mass loadings of nitrate to the Arkansas River  
905 system (main stem and tributaries) for (c) December 2 2006, and (d) August 10 2008, showing the contrast between  
906 the winter and summer seasons.

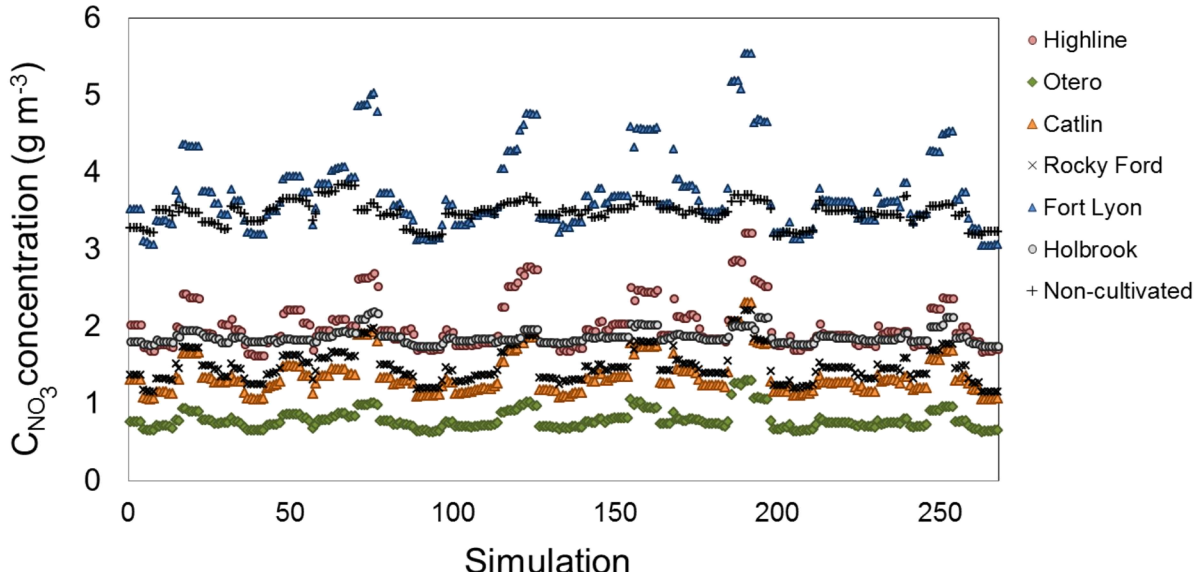
907

908

909

910

*Environmental Factors Governing NO<sub>3</sub> Transport*



911

912 Figure 7. Spatio-temporal average value of  $C_{NO_3}$  in groundwater during the 2006-2009 simulation period for each  
913 canal command area for each of the 280 UZF-RT3D model simulations. The spatio-temporal average for the non-  
914 cultivated areas also is shown (small black crosses).

915

916

917

918

919

920

921

922

923

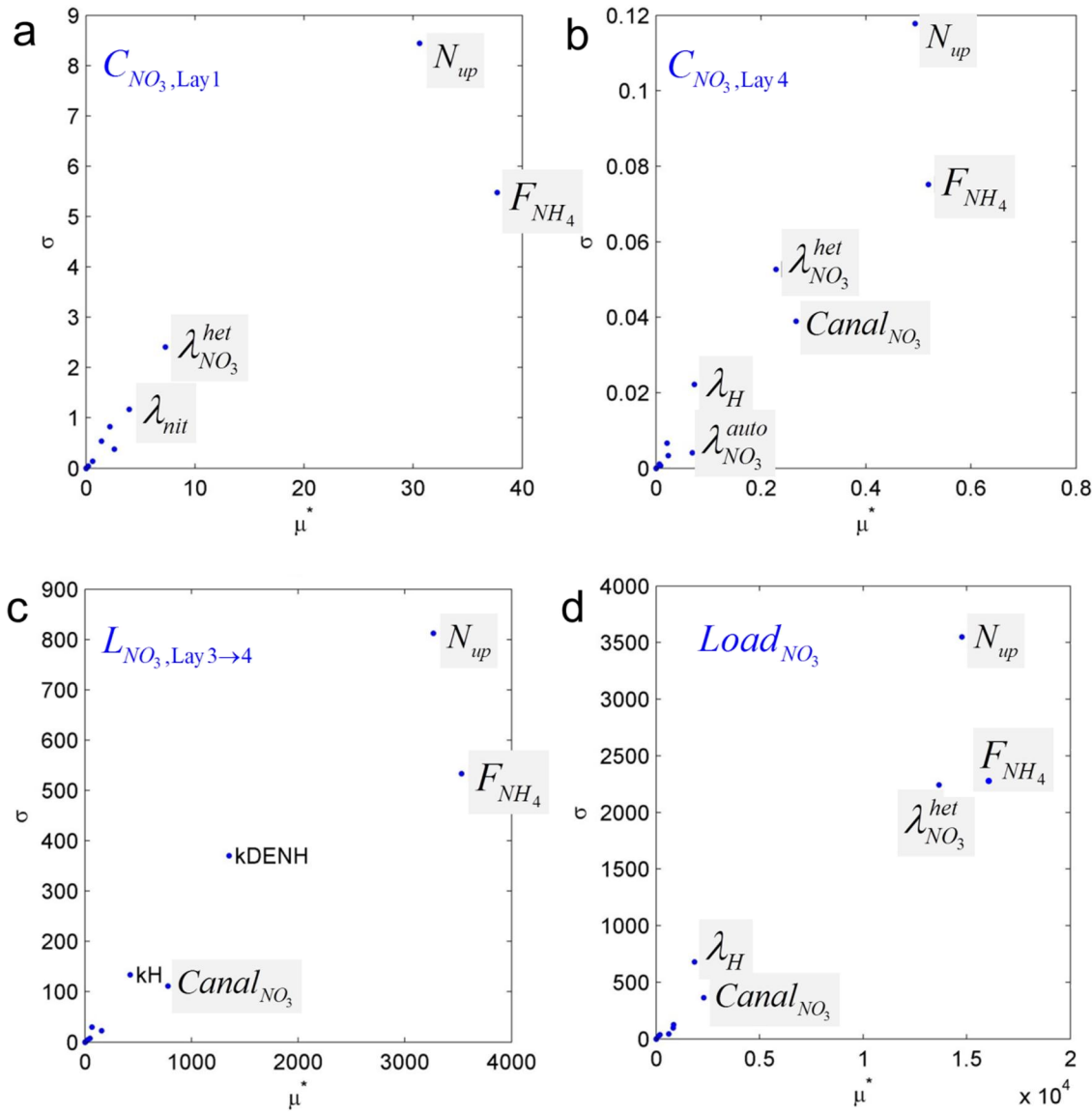
924

925

926

927

928



929

930 Figure 8. Global sensitivity plots ( $\sigma$  vs.  $\mu^*$ ) showing influence of the 9 targeted model input factors on (a)  $C_{NO_3}$  in  
 931 Layer 1 of the model (top 0.5 m of the root zone), (b)  $C_{NO_3}$  in Layer 4 of the model (shallow saturated zone of the  
 932 aquifer), (c)  $NO_3$  mass leaching from Layer 3 to Layer 4 (unsaturated zone to saturated zone), and (d) total mass  
 933 loading of  $NO_3$  from the aquifer to the Arkansas River.

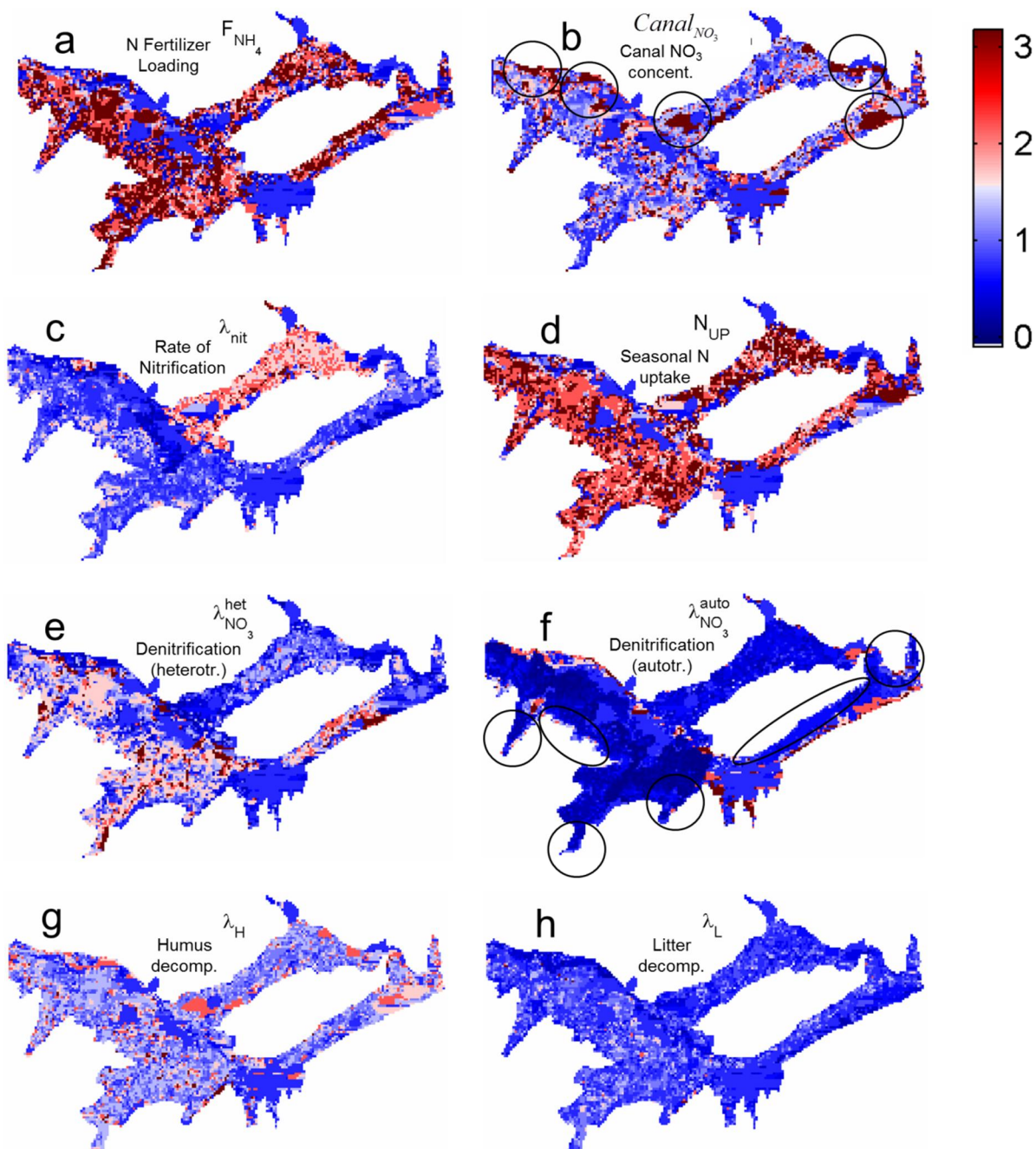
934

935

936

937

*Environmental Factors Governing  $NO_3$  Transport*



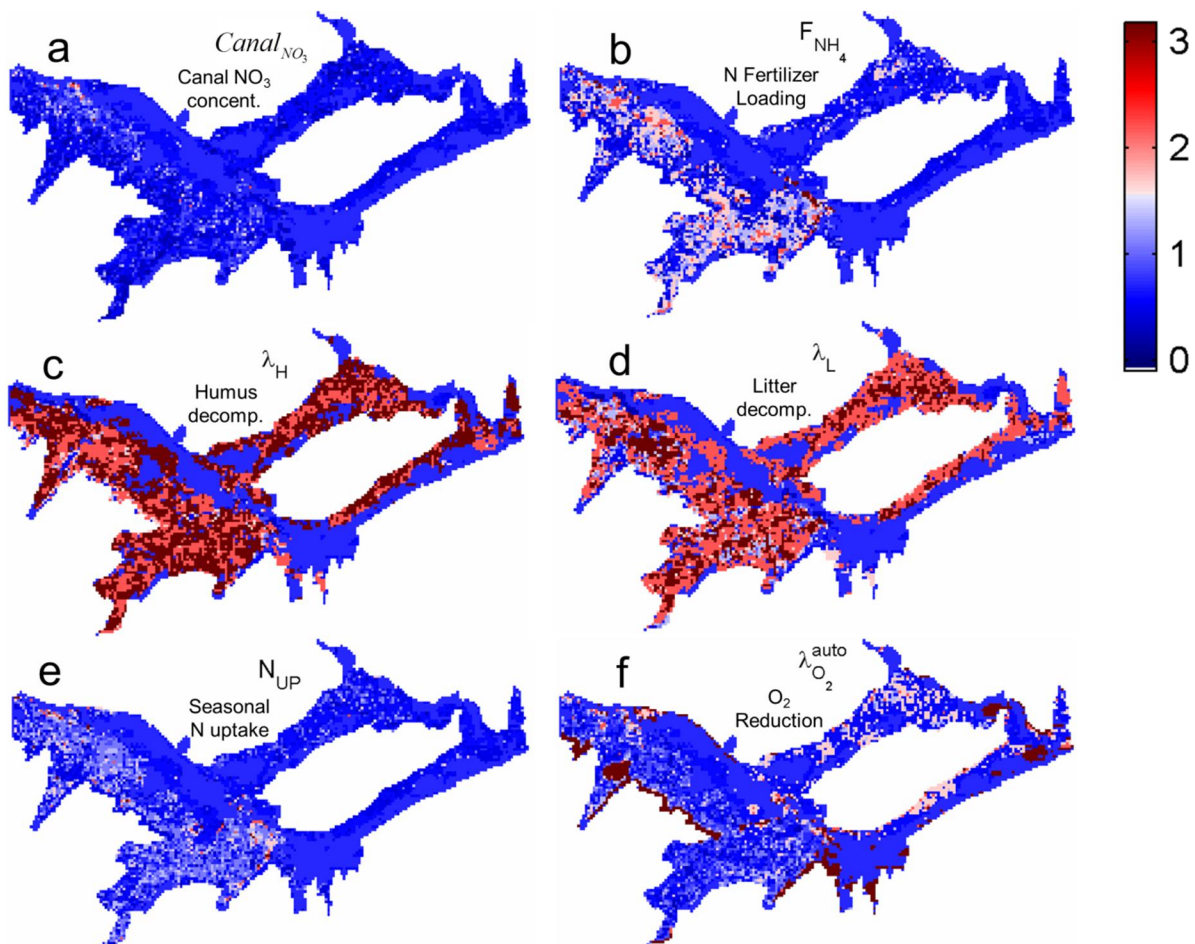
938

939 Figure 9. Cell-by-cell (250 m by 250 m) plots of Savage scores for (a)  $F_{NH_4}$ , (b)  $Canal_{NO_3}$ , (c)  $\lambda_{nit}$ , (d)  $N_{up}$ , (e)  $\lambda_{NO_3}^{het}$ ,  
 940 (f)  $\lambda_{NO_3}^{auto}$ , (g)  $\lambda_H$ , and (h)  $\lambda_L$  indicating the ranking of influence of that parameter on  $C_{NO_3}$  in groundwater for each of  
 941 the 7,776 cells in the study region.

942

943

944



945

946 Figure 10. Cell-by-cell (250 m by 250 m) plots of Savage scores for (a)  $\text{Canal}_{\text{NO}_3}$ , (b)  $F_{\text{NH}_4}$ , (c)  $\lambda_H$ , (d)  $\lambda_L$ , (e)  $N_{\text{UP}}$ , and  
 947 (f)  $\lambda_{\text{O}_2}^{\text{auto}}$ , indicating the ranking of influence of that parameter on  $C_{\text{O}_2}$  in groundwater for each of the 7,776 cells in  
 948 the study region.

949

950

951

952

953